RAIN GAUGE CONCEPT USING S-BAND AND W-BAND FOR ESTIMATION OF MODERATE TO HEAVY PRECIPITATION

By
Leyda León

A thesis submitted in partial fulfillment of the requirements for the degree of

MASTER OF SCIENCE
In
Electrical Engineering

UNIVERSITY OF PUERTO RICO
MAYAGUEZ CAMPUS
2004

Approved by:

_____	_____
Sandra Cruz Pol, PhD. President, Graduate Committee	Date
_____	_____
Stephen Sekelsky, PhD. Member, Graduate Committee	Date
_____	_____
José Colom-Ustáriz, PhD. Member, Graduate Committee	Date
_____	_____
Miguel Vélez Reyes, PhD. Member, Graduate Committee	Date
_____	_____
Héctor J. Jiménez, PhD. Graduate School Representative	Date
_____	_____
Jorge Ortiz Álvarez, PhD. Chairperson of the Department	Date

ABSTRACT

In this research, two Doppler radars working at W-band (95GHz) and at S-band (2.8GHz) together with radiosonde observations (RaOb) were used to retrieve physical parameters such as rainfall rate and vertical air motion (W_t) in rain. These instruments were deployed at the U.S. Department of Energy Atmospheric Radiation Measurement (DOE ARM) Cloud and Radiation Testbed (CART) site in Lamont, Oklahoma where rain data was collected on November 8, 2001 at hour 21:00:17 UTC. In order to retrieve these parameters, the data was processed and analyzed following an iterative method similar to that proposed by Firda [*Firda et al.*, 1999, *Firda* 1997], but using the Marshall-Palmer drop size distribution and a lower non-attenuating frequency, to consider higher rainfall rates. This iterative method includes the use of Liebe's model for suspended water droplets, Mie scattering theory, Green's raindrops shape model and the ideal gas model. Rainfall rates were found to go from 0 mm/hr to 69.9 mm/hr. Vertical air motion was retrieved and values described updraft up to 2.5 m/s and downdrafts up to -1.2 m/s.

RESUMEN

En esta investigación, se utilizaron dos radares Doppler que trabajan en las bandas W (95GHz) y S (2.8GHz) junto con datos obtenidos por las observaciones de radiosondas para obtener parámetros físicos como las razones de lluvia y el movimiento vertical del aire de un evento de lluvia. Estos instrumentos se encuentran en el Cloud and Radiation Testbed (CART) en Lamont, Oklahoma, en donde datos de lluvia fueron obtenidos el 8 de noviembre de 2001 a las 21:00:17 UTC. Para obtener estos parámetros, los datos fueron procesados y analizados siguiendo un método similar al propuesto por Firda [*Firda et al.*, 1999; *Firda,* 1997] pero usando el modelo de Marshall-Palmer para la distribución de tamaño de gotas y una frecuencia no atenuante más baja para considerar lluvia más fuerte. Este método incluye el uso de modelos tales como el modelo de Liebe para gotas de agua, la teoría de Mie, el modelo de Green y el modelo de gas ideal. Fueron encontrados que los valores de razones de lluvia fluctuaban entre los 0 mm/hr y los 69.2 mm/hr. El movimiento vertical del aire fue obtenido y los valores variaban entre los -1.2 m/s y 2.5 m/s.

To Life...

ACKNOWLEDGEMENTS

First of all, I would like to thank GOD. You've being always by my side. I have felt You in the air I breath, in the heartbeats that keep me alive, and in my silence. Thanks for giving me the health to keep going, the opportunity to born in a wonderful family, and to put angels in my way to dry my tears and share my smiles. Thanks for teaching me in every experience I have learned that everything is too small compared to Your Greatness. Thanks for loving me.

I would like to give special thanks to Professor Sandra Cruz-Pol for being a role model to me. She had motivated and encouraged me to continue with graduate studies since I started to work with her as an undergraduate student in 1999. Thanks to Professor Stephen M. Sekelsky from the University of Massachussets who gave me the opportunity to work in this project and have guided me through all the research. Also I would like to thank Professor José Colom, and Professor Miguel Vélez for being part of my graduate committee.

Thanks to Lihua Li, and Steve Sekelsky for providing me assistance during my Summer Internship at the Microwave Remote Sensing Laboratory (MIRSL) and Christopher Williams from the National Atmospheric and Oceanic Administration (NOAA) Aeronomy Laboratory who have helped me a lot through all the research with the data processing.

I would like to thank the Microwave Remote Sensing Laboratory (MIRSL) at the University of Massachussets, the Cloud Microwave Measurements of Atmospheric Phenomena (CLiMMATE) (NASA grant number NAG-102074), Tropical Center for

Earth and Space Studies (TCESS) (NASA grant number EEC-9986821), and the Center for Subsurface Sensing and Imaging Systems (CenSSIS) at the University of Puerto Rico, which provided the funding and the resources for the development of this research.

Finally, I would like to thank my family and friends for their support through all my life. You have always believed in me and supported me every single moment. Thanks Aunt Sylvia for teaching me to always believe in the Divine Order. Thanks to my husband Robert for loving me, encourange and support me in all my present and future plans and to my son Robert Enrique for being my new inspiration. And very special thanks to my mother for being always an example of success and to my dad for teaching me to never look back. Thanks for raising me with love and support. I would not be here without you. I LOVE YOU ALL!

TABLE OF CONTENT

LIST OF TABLES

LIST OF FIGURES

APPENDICES LISTS

CHAPTER 1

INTRODUCTION

The goal of this research is to retrieve the rainfall rate and vertical air motion from the reflectivity obtained in the Doppler spectra by comparing the measurements with simulation. This document presents an iterative procedure that uses the dual frequency method to retrieve rainfall rate, drop size distribution (DSD) and vertical air motion (w_t) in heavy rain events.

For this research two different profilers[1] were used: the University of Massachusetts (UMASS) W-band cloud profiling radar and the National Oceanographic and Atmospheric Administration (NOAA) S-band profiler. Both were deployed at the Cloud and Radiation Testbed (CART) site in Lamont, Oklahoma for a period of 6 months, starting on June 2001, during which weather was monitored and rain data was collected (http://abyss.ecs.umass.edu/Wband2001) for November 8, 2001. Radiosonde observations (RaOb) data was used to obtain several parameters using Liebe's model [*Liebe,* 1989] for suspended water droplets and Mie scattering theory. Green's model [*Green,* 1975] to approximate large raindrop shapes will be used and the ideal gas model will be used to introduce an air density correction factor to take into account the variation in pressure with height.

[1] A profiler is a vertically oriented Doppler radar.

1.1 Motivation

The drop size distribution (DSD) is the most fundamental component in microwave rainfall estimation techniques since it governs all the microwave and rainfall integral relations. It is characterized by a high temporal and spatial variability that affects both microwave measurements and ground validation. Therefore, its accurate estimation for all rain-rates is necessary in order to develop and validate rainfall retrieval algorithms [*Rincon and Lang,* 2002].

The most direct way to measure rainfall rates is using a tipping or weigh bucket rain gauge. While these devices take measurements limited to a point, events like wind introduce errors of approximately 5 to 10% [*Doviak and Zrnic,* 1993]. In the other hand, to get an accurate estimation of rainfall over a large area, the rain gauge network idea have been performed but this still depends upon the rain gauges density over the area and the precipitation spatial variability. In the other way, the use of multi-frequency radar's Doppler Spectrum to study different aspects of precipitation has demonstrated its utility as an accurate profiling rain gauge [*Firda et al.*, 1997]. This does not mean that a sufficiently dense gauges network can measure rainfall rates accurately; in fact, their measurements are used as standard to compare with other techniques. On the other hand, the radar rainfall rates measurement technique has the big advantage to evaluate remotely large areas and to get big sets of data per minute.

Recent studies used the active rain gauge concept to retrieve the DSD and vertical air motion (w_t) in rain using a dual-frequency Cloud Profiling Radar System (CPRS), which operates at 33GHz (Ka-band) and 95GHz (W-band). A previous study was made for low to moderate rain-rates because the use of the Ka-band frequency limited the measurements' accuracy for high rain-rates (heavy rain) due to the attenuation the Ka-band suffers while the signal passes through the rain [*Firda et al.*, 1999]. Using a non-attenuating frequency, such as 2.8GHz instead of the Ka-band, can provide measurements over a wider dynamic range extending the active rain gauge concept to higher rain-rates. The W-band signal will still be used to provide accurate measurement of the vertical air motion in rain. In addition, the fact about the actual drop's shapes, which are no longer spheres, must be considered for heavy raindrops. This fact will be considered using a model that approximates these raindrops' shapes to spheres.

Precipitation data is one of the important inputs to global hydrological cycle and climate models. The dataset currently obtained from the NASA Global Precipitation Climatology Project (GPCP) rain gauge measurements consist of monthly gridded area-mean rainfall totals for a period of time from January 1986 through March 1999. NASA GPCP aims to derive gridded data sets of monthly precipitation totals covering the entire globe based on all available observation technologies and data[2]. This work could potentially be used as a basis for verification of climate model simulations, investigations over global hydrological cycle or as validation for missions such as the GPCP.

[2] http://daac.gsfc.nasa.gov/CAMPAIGN_DOCS/FTP_SITE/INT_DIS/readmes/gpcc.html#404

Literature Review

The knowledge about the inner processes of rain development can be examined by studying the rain DSD. In the past, several research studies have been conducted about this matter including the use of ground-base vertically oriented Doppler radar spectra [*Firda et al.*, 1999; *Firda,* 1997; *Hogan,* 2000]. The Doppler radar spectra method relates the drop-size distribution and the terminal velocity but the w_t introduces errors by shifting the Doppler spectra along the velocity axis. This makes it difficult to measure the terminal velocity independently from the w_t.

The first approach to remove the vertical air motion was the lower bound method. This method assumes the existence of a large number of drops with a minimum detectable size associated to a minimum detectable velocity that can be compared to the measured values to extract the w_t effect, but this method has several complications including the assumption of a large number of drops, the noise effect, the limitation of dynamic range and that the turbulence was not taken into account. These limitations lead to another approach; this time using measured reflectivity to predict the drops' correspondent velocities, but errors mislead to the correct distribution retrieval. Another way to remove the w_t used three parameters to get the drop-size distribution, but it only functioned when turbulence was negligible. The wind profilers were used to obtain the drop-size distribution but this method was limited to low rain rates and uniform wind

fields. All of the approaches named above, were limited to negligible turbulence effects and uniform wind fields [*Firda et al.*; 1999, *Firda* 1997].

Millimeter-wave radars have the potential to estimate vertical winds in rain where complex wind fields exist, even in convective situation where changes in wind and drop size distribution occur rapidly [*Lhermitte* 1988]. The Mie scattering effect, in which case the raindrops diameter is comparable to the radar's wavelength, observed using millimeter-waves extract information of the particles of varied sizes and the distribution as well. In 1988, Lhermitte proposed a method using the Mie backscattering null observed in the 94GHz Doppler spectra to determine the vertical air motion [*Lhermitte* 1988]. This algorithm uses correlation analyses between the measured and simulated spectra to remove the vertical air motion and the turbulent broadening even where complex wind fields and turbulence is present, different from the previous four approaches.

In 1999, Lhermitte's proposed algorithm was applied to measurements collected by dual-frequency CPRS (with 35GHz and 95GHz channels) to obtain the Doppler spectra. This approach to retrieve the drop-size distribution was successful but was limited for low-rain rates because of the Ka-band attenuation through the precipitation cloud [*Firda et al.*, 1999; *Firda* 1997].

Extending our study to all rain rates will require the use of a lower frequency, S-band non-attenuating radar and take into account the real drop's shape. For heavy rain, the drop sphericity is not hold because the change in shape due of its weight and collisions with other drops while falling. This situation will be tackled using Green's model, which approximates the drop shape as a more realistic oblate spheroid [*Green* 1975].

1.3 Summary

The following chapters present detailed the theory and methodology used during this research. The last chapters as well, present the results and conclusions.

Chapter 2 present the background theory needed to understand the methodology to be followed. It discussed the precipitation formation and introduces weather Doppler radar measurements. In the other hand the Doppler spectra is discussed in all its parts including the Mie scattering theory, the raindrops size distribution, the velocity-diameter relation and the measurement biases. Also the radiosonde observation utility is explained as well and the Liebe's Model for suspended water droplets and the air density correction factor.

The following chapter, Chapter 3, is dedicated to the methodology. This is explained step by step, including the experiment setup, the data collection process and the data processing as well.

Last chapters, Chapters 4 and 5, present the results and conclusions obtained from the data process and methodology. The situations like the data aliasing and alignment are carefully explained and presented. In addition, the dual-frequency-method results are presented such as the rainfall rates, and the vertical air motion (w_t) estimates for several time profiles and range gates.

CHAPTER 2

BACKGROUND THEORY

2.1 Weather Doppler Radars

Doppler Radars have an important role in the field of meteorology. These sensors send out electromagnetic pulses that interact with objects in the path of the signal, such as water droplets, that scatters and absorb the electromagnetic energy. Fortunately, microwave radiation is mostly scattered by targets. For monostatic (single antenna) radars, the received signal is the backscattered radiation. This signal provides valuable information about the target's velocity and reflectivity, which in advanced Doppler radar technology, are obtained with high resolution, being vital to short-term forecasting and severe weather prediction.

2.1.1 Radar Equation

The radar equation describes the relationship between the average power of the received signal and the properties of the scattering volume, located at a distance *r*, as a function of the radar equipment's technical characteristics, and the conditions of propagation between the radar and its target. For distributed targets such as rain precipitation (see Figure 2.1), the radar has a distributed volume filling its pulse volume such that,

$$\overline{P_r} = \frac{P_t G_o^2 \lambda^2 L_r L^2 \eta}{(4\pi)^3} \int_V \frac{\left| f_\eta(\theta,\phi) \right|^4}{r^4} dV \tag{1}$$

where P_r is the average received power, P_t is the transmitted power, G_o^2 is the radar's antenna gain, L_r is the loss due to the finite width of the pass band of the receiver, L^2 is the attenuation on the radar-target path, η is the radar reflectivity factor in $m^2\ m^{-3}$, $\left| f_\eta(\theta,\phi) \right|^4$ is the power density pattern, and V is the volume of integration of the pulse with $dV=r^2 dr d\Omega$. When r is large compared to the resolution volume $\frac{c\tau}{2}$ with $dr \approx \frac{c\tau}{2}$ then we have,

$$\overline{P_r} = \frac{P_t G_o^2 \lambda^2 L_r L^2}{(4\pi)^3} \frac{c\tau}{2} \frac{\eta}{r^2} \int_\Omega \left| f_\eta(\theta,\phi) \right|^4 d\Omega \tag{2}$$

Assuming that the power distribution in the main lobe can be represented by a Gaussian function then the integral part of equation 2 can be derived.

$$\int_\Omega \left| f_\eta(\theta,\phi) \right|^4 d\Omega = \frac{\pi \theta_o \phi_o}{8 \ln 2} \tag{3}$$

Finally the radar equation can be described as,

$$\overline{P_r} = \frac{P_t G_o^2 \lambda^2 L_r \theta_o \phi_o c\tau}{1024 \pi^2 \ln 2} L^2 \frac{\eta}{r^2}, \tag{4}$$

where ϕ_o and θ_o are the 3-dB beam widths. This equation can be rearranged in the form

$$\overline{P_r} = C L^2 \frac{\eta}{r^2}, \tag{5}$$

where C is known as the radar constant and only depends upon the radar technical characteristics.

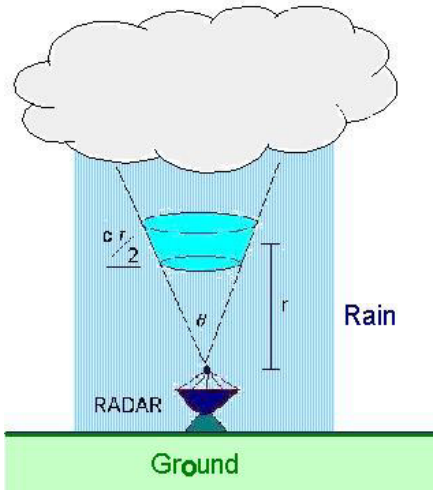

Figure 2.1: Vertically oriented Doppler radar measuring a rain event.

2.1.2 Pulse Pair and Fast Fourier Transform Techniques

When the radar receives echoes from the backscattered energy of a distributed target, it does so as a sequence of complex voltages samples as described in equation 6. One component is associated with the signal and the other with white noise, where s_k is the amplitude of the kth signal, w_d is the Doppler phase shift associated with a moving target within the volume, T_s is the spacing between the echoes and n_k is the white noise.

$$V(kT_s) = s_k e^{(jw_d kT_s)} + n_k \tag{6}$$

Knowing the sequence of complex voltages, an autocorrelation function of the signal samples can be constructed.

$$R(mT_s) = E\left\{V^*(kTs)V((k+m)T_s)\right\} \tag{7}$$

Considering that Doppler spectra from weather signals follow a Gaussian distribution (see equation 8) the autocorrelation function takes the form of equation 9

$$S(v) = \frac{\bar{S}}{\sqrt{2\pi\sigma_v^2}} e^{\frac{-(v-\bar{v})^2}{2\sigma_v^2}} + \frac{2NTs}{\lambda} \tag{8}$$

$$R(mTs) = \bar{S} e^{-8\left(\frac{\pi\sigma_v mTs}{\lambda}\right)^2} e^{\frac{-j4\pi\bar{v}mT_s}{\lambda}} + N\delta_m \tag{9}$$

In equation 9, $\bar{S}$ is the mean signal power, $\bar{v}$ is the mean velocity, σ_v is the spectral width, N is the mean white noise power, and δ_m is 1 for m=0, and 0 otherwise [*Doviak and Zrnic* 1993, *Bringni and Chandrasekar* 2001]. It can be observed from equation 8 that the higher the spectral width the narrower the Doppler power spectra would be, but wider the magnitude of the autocorrelation function (see equation 9). Also the argument of the autocorrelation function gives information about the mean velocity detected.

To estimate the Doppler spectral parameters such as the weather signal power, mean velocity, the spectral width two different techniques can be applied. These are the Pulse Pairs technique and the Fast Fourier Transform technique. The latter is commonly used to estimate the whole power spectrum.

The Pulse-Pair signal processing algorithm estimates the first and second moments of the Doppler Spectra by calculating the auto-correlation function at a time delay of *T=1/PRF* (pulse repetition frequency) [*Doviak and Zrnic* 1993]. The first moment corresponds to the mean Doppler velocity and the second moment corresponds to the

spectral width. Therefore with this technique it is possible to have the three most important quantities in weather signals, the weather signal power, the mean Doppler velocity, and the spectral width.

The Fast Fourier technique estimates the full Doppler spectrum by computing the Fast Fourier transforms (FFT) to the auto-correlation function. This is represented in equation 10.

$$S(v) = \sum_{i=0}^{M-1} R(i) e^{\frac{-j2\pi vTs}{\lambda}} \tag{10}$$

The first and second spectral moments using the FFT technique are described in equations 11 and 12.

$$\hat{v} = \sum_{k=-M/2}^{M/2} v(k) S(k) \tag{11}$$

$$\hat{\sigma}_v = \sum_{k=-M/2}^{M/2} (v(k) - \hat{v})^2 S(k) \tag{12}$$

The Pulse-Pair mode produces less information because it calculates an average reflectivity for each one of the profile's cells, while the FFT mode produces a large volume of data because it saves the complete Doppler spectrum for each range cell. It is our interest to obtain the complete power spectrum; therefore data is collected in FFT mode.

2.2 Rain Precipitation Doppler Spectra

2.2.1 Doppler Spectra

The Doppler spectrum data collected by both profilers using the FFT mode is obtained from the power spectrum created by the backscattered energy and the velocity. This provides information about the drop size distribution with the terminal velocity of the hydrometeors. This relation with the Doppler spectra is as follows,

$$S(v) = N(D)\sigma_b(D)(dD/dv) \qquad [\text{mm}^2\text{m}^{-3}/\text{m}*\text{s}^{-1}] \qquad (13)$$

where v is the velocity of each drop, $S(v)$ is the Doppler spectra, which quantifies how much power is received from each velocity range, $N(D)$ is the drop size distribution (how many drops exist of each size per given volume), $\sigma_b(D)$ is the backscatter cross section of a drop of diameter D, and dD/dv is the relationship between the drops' diameter and terminal velocity.

2.2.2 Mie Scattering

The radar measures the backscatter energy received from the volume of raindrops. There is one basic theory describing this scattering, the Mie scattering theory. As a special case of Mie theory, the Rayleigh scattering describes scattering characteristics of particles that are much smaller than the wavelength of radiation that they encounter. Objects of this size do not scatter all wavelengths evenly. Alternately, Mie scatterers are larger in size and are able to scatter all wavelengths in all directions with measurements

that give an estimate of the particle's size (comparable to the radiation wavelength) with the backscattering coefficient $\sigma_b \propto f^4$ [*Ulaby et al.*, 1986]. For instance, precipitation droplets have the size to act as Mie scatterers at our operating frequency. Water droplets tend to have a high efficiency for scattering.

The Doppler spectrum *S(v)* in equation 13 is related to the backscatter cross section where $\sigma_b(D)$ is in (mm^2). For our simulations of the backscatter and extinction cross sections (σ_b and σ_e) we use the formulas described in equations 14 and 15.

$$\sigma_b(D) = \xi_b \pi r^2, \qquad [\text{mm}^2] \tag{14}$$

$$\sigma_e(D) = \xi_e \pi r^2 \qquad [\text{mm}^2] \tag{15}$$

derived from Mie's solution for the scattering and absorption of electromagnetic waves by a dielectric sphere of arbitrary radius r in mm. The variables ξ_b and ξ_e are the backscattering and extinction efficiencies, respectively.

First, the values of ξ_b and ξ_e are obtained, then σ_b and σ_e are simulated. From Mie's solution, the backscattering efficiency is given by

$$\xi_b = \frac{1}{\chi^2}\left|\sum_{l=1}^{\infty}(-1)^l(2l+1)(a_l + b_l)\right|^2, \tag{16}$$

and the extinction efficiency is given by

$$\xi_e = \frac{2}{\chi^2}\sum_{l=1}^{\infty}(2l+1)\,\mathrm{Re}\{a_l + b_l\}, \tag{17}$$

where Re means "the real part of", and a_l and b_l are the Mie coefficients. These coefficients are formulated in terms of

$$\chi = \frac{2\pi r}{\lambda_0}\sqrt{\varepsilon_{rb}^{'}}\,, \tag{18}$$

which is the particle size with respect to the free-space wavelength λ_0 in mm, where $\varepsilon_{rb}^{'}$ is the real part of the relative dielectric constant of the background medium. When the background medium is air, as is true in the atmosphere, then $\varepsilon_{rb}^{'} = 1$. Mie coefficients are also formulated in terms of

$$n = \sqrt{\varepsilon}\,, \tag{19}$$

which is the refraction index, calculated in terms of ε, the permittivity for liquid water.

The expressions for a_l and b_l are

$$a_l = \frac{\left(\frac{A_l}{n} + \frac{1}{\chi}\right)\mathrm{Re}\{W_l\} - \mathrm{Re}\{W_{l-1}\}}{\left(\frac{A_l}{n} + \frac{l}{\chi}\right)W_l - W_{l-1}} \tag{20}$$

and

$$b_l = \frac{\left(nA_l + \frac{1}{\chi}\right)\mathrm{Re}\{W_l\} - \mathrm{Re}\{W_{l-1}\}}{(nA_l + \frac{1}{\chi})W_l - W_{l-1}}, \tag{21}$$

where

$$W_l = \left(\frac{2l-1}{\chi}\right)W_{l-1} - W_{l-2}\,, \tag{22}$$

and

$$W_0 = \sin\chi + j\cos\chi \tag{23}$$

2.2.3 Raindrop Size Distribution

One way in order to have rain is having a cloud made up of water droplets in the air best known as water vapor. Along with this water are tiny particles called condensation nuclei (for example salt leftover after sea water evaporates, or a particle of dust or smoke). Condensation occurs when the water vapor wraps itself around the tiny particles. Each particle (surrounded by water) becomes a tiny droplet between 0.001 and 0.05 millimeter in diameter. However, these droplets are too light to fall out of the sky. For these tiny droplets to fall, one droplet has to collide with another droplet, the bigger droplet will fuse with the smaller droplet making a larger drop. This new bigger droplet will collide with smaller droplets and become even bigger; this is called coalescence (see Figure 2.2). Soon the droplet is so heavy that the cloud can no longer hold it up and it starts falling. As it falls it fuses with even more droplets. As soon as the droplet reaches the size of 0.5mm in diameter or bigger, it is considered a raindrop (see Table 2.1 for typical raindrop sizes). Drops larger than 5.8 to 6 millimeters will usually split into two separate drops [*Doviak and Zrnic* 1993; *Sauvegnot* 1992; *Bringi and Chandrasekar* 2001].

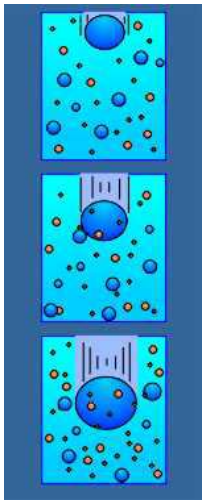

Figure 2.2: Collision-Coalescence process in rain precipitation events.

Table 2.1: Typical drop's size and their fall velocities for several types of rain event intensities [*Rogers and Yau* 1989].

Rain Type	**Drop Size [mm]**		**Terminal Velocity[m/s]**
Light Stratiform Rain (RR > 2.54 mm/hr)	Small Drop	0.5	2.06
	Large Drop	2	6.49
Moderate Stratiform Rain 2.794 < RR < 7.62 mm/hr	Small Drop	1	4.03
	Large Drop	2.6	7.57
HeavyRain RR > 7.62 mm/hr Or Thundershower RR≈ 25.4mm/hr	Small Drop	1.2	4.64
	Large Drop	4	8.83
	Largest Possible	5	9.09s
SMALL Raindrop		**LARGE Raindrop**	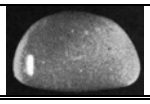

The raindrop will continue falling until it reaches the ground. As it falls, sometimes a gust of wind (updraft) will force the drop back up into the cloud where it continues eating other droplets and getting bigger. When the drops finally reach the ground, the biggest drops will be the ones that bumped into and coalesced with the most droplets. The smaller drops are the ones that didn't run into as many droplets. Raindrops are different

sizes for two primary reasons: the condensation nuclei size and the different rates of collision-coalescence process [*Lutgens and Tarbuck* 1988].

The size distribution of hydrometeors have been of great importance in order to study the inner process of weather events development such as rain, and for determining parameters such as rain-rate, reflectivity and water content. This distribution describes the volume density of hydrometeors per unit of diameter, i.e. how many particles of a specific diameter exist over a determined volume. In 1948 J.S. Marshall and McK. Palmer empirically determined the density of raindrop diameters at a surface using dyed filter paper [*Marshall and Palmer* 1948].

For rain, the drop size distribution can be described as a special case of the gamma distribution given by equation 24 described by Ulbrich in 1983, where $-3 \leq \mu \leq 8$ [*Ulbrich* 1983].

$$N(D) = N_o D^{\mu} e^{-\Lambda D} \qquad [\text{mm}^{-3}\text{mm}^{-1}] \qquad (24)$$

In rain's case μ=0 and it is known as the exponential distribution and can be described as,

$$N(D) = N_o e^{-aR^b D} \qquad [\text{mm}^{-3}\text{mm}^{-1}] \qquad (25)$$

According to the Marshall-Palmer drop size distribution, *a* and *b*, that determines the distribution's slope and are given by 4100 and –0.21 respectively, N_o= 8 x 10^6 m^{-4}, and the raindrops diameter, *D*, is in m [*Marshall and Palmer 1948*].

2.2.4 Velocity-Diameter Relation

When hydrometeors fall, equilibrium quickly establishes between two forces, gravity (downward) and aerodynamic drag (upward). The resulting velocity is called the terminal velocity, or simply fall speed, v_T. In 1949, Gunn and Kinzer empirically determined a relationship between a water drop's velocity and its diameter in stagnant air at sea level [*Gunn and Kinzer* 1949]. This relationship is commonly used to calculate the rainfall rate on the ground using *N(D)* and to derive the Doppler velocity power spectra for vertically oriented Doppler radars. This velocity-diameter relationship is given as,

$$v(D) = 9.25\left[1\text{-}e^{(-6.8D^2 - 4.88D)}\right] \qquad \text{[m/s]} \qquad (26)$$

where *v(D)* is in m/s and *D* is in cm. This formula is valid for diameters ranging from 0.5 to 6 mm to have an acceptable fit. This formula must be corrected to account for the air density decrease as the altitude increases. Several other relations have been developed like the ones of Atlas (1973) and Atlas-Ulbrich (1977) which are valid for $0.6 \le D \le 5.8$ mm and $0.5 \le D \le 5$ mm respectively, and both has an acceptable fit over the Gunn-Kinzer 1949 relationship [*Foote and duToit* 1969].

2.2.5 Drops' Shape Effect (Green's Model)

When rain falls, their huge amounts of drops have different sizes causing them to fall at slightly different speeds. As a consequence of the differing drop speeds, there are many collisions among raindrops. Some collisions cause distortions in the drops' shapes as they bounce off one another (see Figure 2.2). Other collisions cause drops to coalesce,

forming a larger drop in the process. And some collisions cause drops to break apart into smaller drops. As the drops change their size, they come through a variety of spherical distortions with flattened bases and rounded tops, looking more like falling oblate spheroids rather than teardrops, as they fall. This distortion is caused by the surface tension of the water and the pressure of the air pushing up against the bottom of the drop as they descend, which flattens the lower drop surface. This aerodynamic drag force can further deform larger drops into oblate spheroids shapes, causing the biggest ones (around $D > 5$ mm) to eventually split into two or more smaller drops.

This factor is considered using A. W. Green's model [*Green* 1975]. This model explains how the drop deviates from sphericity as the drops collide with other drops increasing in size and changing from spheres to oblate drops. We relate the sphere diameter $D=2a_0$ and the minor and major axis a and b of the equivalent volume ellipsoid, where a represents the diameter obtained in cm (see equations 27a, 27b and Figure 2.3).

$$\left(\frac{a}{ao}\right)^2 - 1 = \frac{4}{17}\left(\sqrt{\frac{17B}{4}+1} - 1\right) \tag{27a}$$

$$\frac{b}{a} = \left[\frac{4}{17}\sqrt{\frac{17B}{4}+1} + \frac{13}{17}\right]^{-3/2} \tag{27b}$$

where $B=\rho a_o^2 g' \sigma^{-1}$ is the Bond number, which is the ratio of the drag and surface forces at terminal speed. The surface tension is $\sigma = 72.75$ g/s^2, the effective gravity is $g'=980$ cm/s^2, and the water density is $\rho=0.998$ g/cm^3 are used in the Bond number calculation.

To represent equation 27a an 27b in terms of the particle's diammeter and the axial ration b/a, equation 28 can be formulated.

$$D = 2\left(\frac{\sigma}{g'\rho}\right)^{1/2} \frac{\left[(b/a)^{-2} - 2(b/a)^{-1/3} + 1\right]^{1/2}}{(b/a)^{1/6}} \tag{28}$$

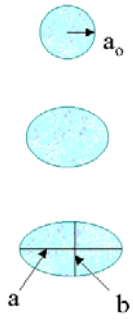

Figure 2.3: Side views of ellipsoids and the equivalent sphere used in Greens model for large raindrops such as those found in heavy rain.

A more accurate model for drop shape can be found in Bringi and Chandrasekar 2001. It mentions Beard and Chuang 1987 model that includes the aerodynamic effects present in raindrop fall. This model yields to equation 29 is valid for $0 \le D \le 7.0$ mm.

$$\frac{b}{a} = 1.0048 + 5.7\times10^{-4} D - 2.628\times10^{-2} D^2 + 3.682\times10^{-3} D^3 - 1.677\times10^{-4} D^4 \tag{29}$$

A more accurate model for diammeters from $1 \le D \le 4.0$ mm was developed by Andsager et al. 1999. This model provided a fit to all the laboratory data and Chandrasekar et al.1988 data yielding to equation 30 [*Bringi and Chandrasekar* 2001].

$$\frac{b}{a} = 1.012 - 0.01445\, D - 0.01028\, D^2 \tag{30}$$

2.2.6 Measurement Biases

A bias is a systematic difference between an estimate and the true value of a parameter [*Doviak and Zrnic* 1993; *Sauvegnot* 1992; *Firda et al.*, 1999; *Firda* 1997]. Vertical air motion (updrafts and downdrafts) and turbulence, both bias the measured signal. These effects must be removed from the radar data to obtain an accurate drop size distribution.

2.2.6.1 Vertical Air Motion (W_t)

Often the vertical air motion of the atmospheric volume sampled by the radar beam contaminates the observed mean Doppler velocity that can be detected as a spectrum shift as shown in Figure 2.4. The dual-frequency method uses the Mie scattering null-effect observed at microwave frequencies to remove biases due to the vertical air motion. Lhermitte's work showed that the Doppler spectrum depends on frequency; however the drop-size distribution does not. Plotting both frequency spectra (at 95GHz and 33GHz), it follows that the K_a-band has a Gaussian shape and the W-band has several peaks and nulls that later will be used to calculate the w_t locating the first null of the measured and simulated spectra [*Firda et al.*, 1999; *Firda* 1997, *Doviak and Zrnic* 1993]. To retrieve the particle's terminal velocity, equation 28 must be considered.

$$v_d = w_t + v_T \tag{31}$$

where v_d is the Doppler velocity, w_t is the vertical air motion and v_T is the raindrop's terminal velocity, all in m/s.

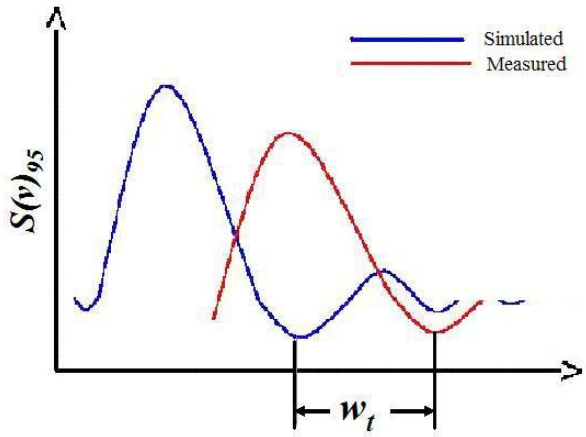

Figure 2.4: Spectrum shifting caused by the vertical air motion.

2.2.7 Reflectivity

The radar reflectivity is the sum of all the backscattering cross sections in a pulse resolution volume divided by the volume [*Sauvegnot* 1992]. This can be described as,

$$\eta = \int_{D_{\min}}^{D_{\max}} N(D)\sigma(D)dD \qquad [\mathrm{mm^2 m^{-3}}] \qquad (32)$$

This parameter is a characteristic quantity of the target but does not mean any assumption of the scattering medium [*Sauvegnot* 1992]. When standard frequencies for meteorological radars are used, Rayleigh condition is considered for which the normalized radar reflectivity factor is defined by

$$\eta = \frac{\pi^5}{\lambda^4}\left|K_w\right|^2 \int_{D\min}^{D\max} D^6 N(D)dD \qquad [\mathrm{mm^2 m^{-3}}] \qquad (33)$$

using the relationship of the backscattering coefficient for Rayleigh condition in equation 29.

$$\sigma_b(D) = \frac{\pi^5}{\lambda^4}|K_w|^2 D^6 \qquad [\text{mm}^2] \qquad (34)$$

The integral part is known as reflectivity Z and is given in mm^6/m^3. When the observed volume does not satisfy the Rayleigh conditions, the value Z is expressed as and equivalent reflectivity factor. This way we have,

$$Z_e = \frac{\lambda^4}{\pi^5|K_w|^2}\eta \qquad [\text{mm}^6\text{m}^{-3}] \qquad (35)$$

Using equations 13, 32 and 35, for both radars the equivalent reflectivity can be determined with equation 36.

$$Z_e = \frac{\lambda^4}{|K_w|^2\pi^5}\int_0^\infty S(v)dv \qquad [\text{mm}^6\text{m}^{-3}] \qquad (36)$$

In all these equations K_w is calculated from the refraction index of water, *S(v)* is the power spectra, v is the terminal velocity and λ is the wavelength of the radar in free space in mm [*Firda et al.*, 1999; *Firda* 1997].

The ratio of both frequencies equivalent reflectivity factors, known as the dual-wavelength ratio, *DWR*, is calculated using equation 37.

$$DWR = 10\log_{10}\left(\frac{Z_{e2.8}}{Z_{e95}}\right) \qquad (37)$$

2.2.8 Attenuation by rain

Along the path traveled by the radar pulse, the amount of transmitted energy dissipates due to the atmosphere and its constituents. This attenuation has to be considered in order to account for the losses between the radar and the target. Two types of attenuation like attenuation by gases and by hydrometeors can be observed. In our case, hydrometeor attenuation by rain precipitation (described in equation 38) at microwave frequencies needs to consider Mie theory to retrieve the extinction cross-section σ_e. This is because eventhough for the longest wavelength of λ=10 cm and a typical raindrop diameter of 0.2 cm the Rayleigh approximation condition of $D \leq \lambda/16$ is valid, this does not apply for all rain conditions. For heavy rain and longer wavelengths (i.e. λ=3 cm and a large raindrop with $D \approx 0.5$cm) Mie scattering solution must be used. Therefore, in general case, Mie scattering is used to compute the extinction cross-section σ_e to calculate attenuation.

The one-way attenuation can be calculated as,

$$K = 4.34 \times 10^3 \int_0^\infty N(D)\sigma_e(D)dD \qquad \text{[dB/km]} \qquad (38)$$

where σ_e is the extinction cross-section in mm^2 and K is in dB/km [*Doviak and Zrnic* 1993; *Firda et al.*, 1999; *Firda* 1997]. To get K in dB/m with D in mm, equation 38 must be multiplied by a factor of 10^{-9}.

2.3 Radiosonde Observations

Radiosonde observations of temperature and pressure are used as inputs to Liebe's Model for suspended water droplets and to calculate the air density correction factor.

2.3.1 Liebe's Model for suspended water droplets

Liebe model [*Liebe* 1989] for suspended water droplets is used to calculate the complex refraction index n_w and the dielectric factor $|K_w|^2$, at both 2.8 and 95 GHz. Both quantities are defined in equation 39 and 40.

$$n_w = \sqrt{\varepsilon} \tag{39}$$

$$|K_w|^2 = \left| \frac{(n_w^2 - 1)}{(n_w^2 + 2)} \right|^2 \tag{40}$$

where $\varepsilon = \varepsilon' - j\,\varepsilon''$ and ε', ε'' are the real and imaginary parts of the relative permittivity for liquid water for a given frequency and temperature. The code for this model is included in the Appendices.

2.3.2 Velocity-Diameter Relation's Air Density Correction

Gunn, R. and Kinzer, G.D. V-D relationship was determined at sea level. For this reason the fact that the droplets terminal velocities increase as altitude increase has to be considered. In 1969 Foote and du Toit examined data of terminal velocities of falling drops in a partially evacuated tube, deducing that terminal velocity dependent on the air density. A correction factor was proposed (equation 41) which has to be multiplied by the V-D equation. This factor, from now on "air density correction factor", is dependent

on the air density at sea level $\rho_o=1.226$ kg/m^3 [*Doviak and Zrnic* 1993; *Sauvegnot* 1992; *Firda et al.*, 1999; *Firda* 1997].

$$(\rho_o/\rho)^{0.4} \tag{41}$$

2.4 Velocity Aliasing

Velocity aliasing can be observed in the data collected by the radar. Due to the discrete sampling of the phase shift there is a maximum frequency or Doppler velocity, which can be retrieved. This maximum unambiguous Doppler velocity (v_{max}) is given by the pulse repetition frequency (PRF) and the wavelength of the radar (see equation 42). If higher velocities are detected they tend to fold up into this maximum interval that can be detected by the radar. Folding can be easily located where the Doppler velocity jumps from one extreme to the other.

$$v_{\max} = f_{PRF}\frac{\lambda}{4} \tag{42}$$

CHAPTER 3

METHODOLOGY

As stated in Chapter 1, the goal of this research is to retrieve the rainfall rate and vertical air motion from the reflectivity obtained in the Doppler spectra by comparing the measurements with simulation. This way attenuation can be corrected and the vertical air motion be removed from the collected data. To accomplish this, collocated data from the two radars must be aligned in time and space (see Figure 3.1) and the rain rate retrieved, for each range cell for all time profiles, by an iterative procedure explained ahead.

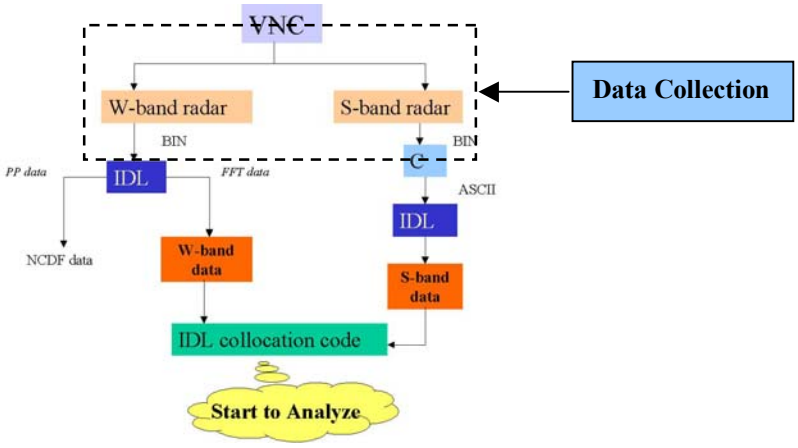

Figure 3.1: Flow diagram depicting steps needed to align data from both radars.

3.1 Experiment Setup

During this research two different profilers were used: the University of Massachusetts (UMASS) W-band cloud profiling radar and the National Oceanographic and Atmospheric Administration (NOAA) S-band profiler (see Figure 3.2). Both were

deployed at the Cloud and Radiation Testbed (CART) site in Lamont, Oklahoma for a period of 6 months, starting on June 2001, during which weather was monitored and rain data was collected (http://abyss.ecs.umass.edu/Wband2001) for November 8, 2001. Radiosonde observations (RaOb) data was used to obtain several parameters using Liebe's model for suspended water droplets and Mie scattering theory. Green's model to approximate large raindrop shapes will be used and the ideal gas model will approximate a correction factor.

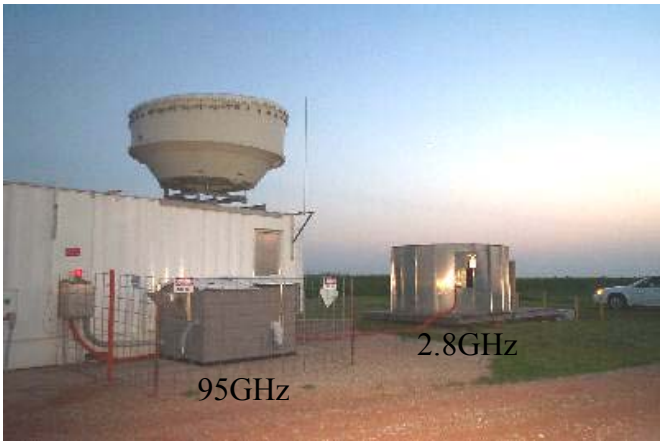

Figure 3.2a: UMASS (95GHz) and NOAA (2.8GHz) radars deployed at the CART site in Lamont, Oklahoma in 2001.

Figure 3.2b: Controlling UMASS (95GHz) and NOAA (2.8GHz) radars, directly from Oklahoma.

3.1.1 S-band Radar

The 2.8GHz NOAA radar uses a vertical-pointing shrouded parabolic reflector antenna, a solid-state transmitter and hardware and software. This profiler was controlled with two computers. One is called the Radar Computer (AL_1_2835) and the other is called Communication Computer (AL_1_DataComm). The Radar Computer controlled and acquired the real data and the Communication Computer communicates with the Radar Computer, communicated with the outside world, and stored the radar data on JAZZ disks (changed periodically by the ARM personnel and shipped to NOAA).

3.1.2 W-band Radar

Four different computers control the 95GHz UMASS radar. A Linux machine was set up to process the data and works as a local network server while it communicates with the outside world using the Virtual Network Computing server (VNC). An HP Linux machine runs the radar operation. This computer controls the data acquisition system and saves the collected data to the RAID storage system that then will be uploaded to the ARM data archives. The Windows Millennium machine (WinMe) records the information status, runs a quality control program and reports any abnormal occurrences. The last and fourth computer involved is a PC104. This computer records the system's "health" measuring components temperatures and voltages, stores images of the web cameras and controls the power switches. Both radars parameters are described in Table 3.1.

Table 3.1: S-band and W-band radars parameters.

Parameter	S-band	W-band
Frequency(GHz)	2.835	94.92
T_x polarization	V	V OR H
R_x polarization	V	V and H
Peak Power(kW)	0.38	1.5
Average Power (W)	7.6	15
Antenna	3m dish with shroud	0.31m lens
2-way 3dB antenna beamwidth (°)	3.2	0.7
Range resolution (m)	60	75
Noise Figure (dB)	2.6	13
dBZ_e (R=1km, 30s)	-40	-59

The W-band radar has a range height resolution of 75 m for each cell measure, while the S-band range cell resolution is of 60 m. This is considered later in aligning both radars' data.

3.1.3 Radiosonde Observations (RaOb)

The Longwave Surface Sonde (LSSonde) observations in the Southern Great Plains (SGP), Cloud and Radiation Testbed (CART) Site, in Lamont, Oklahoma were used. This instrument provides vertical profile measurements of the atmosphere pressure and temperature up to a height of 22 km going in 11 m steps. The starting and ending values of the height values are 315 m and 22,183 km respectively.

A horizontally stratified atmosphere is assumed, where at each atmospheric layer the values obtained from the RaOb such as temperature and pressure are constant. (See Figure 3.3)

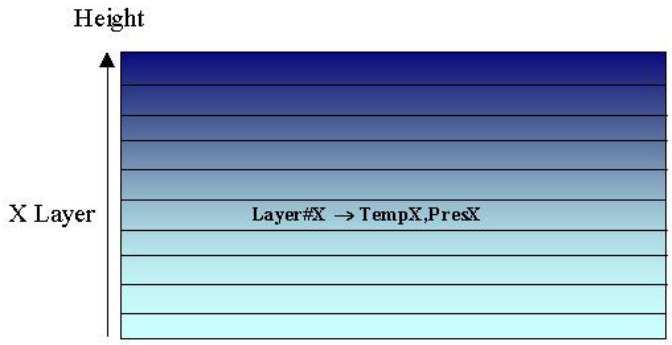

Figure 3.3: Horizontally stratified atmosphere is assumed, where each layers has a constant pressure and temperature.

This temperature information is used to calculate the refractive index at each layer and the both the pressure and temperature are used to compute the air desity correction factor.

3.1.4 Software

The data was processed and analyzed using the Interactive Data Language, IDL, developed by Research. It is an array-oriented language with numerous graphical display techniques.

3.2 Data Collection

The data collection processes consist of different phases as described below. Both radars can work at two different modes. The Pulse-Pair technique is what we

denominated as “Normal Mode” while the Fast Fourier as “Precipitation Mode”. For the study, data was collected in “Precipitation Mode”.

The Virtual Network Computing (VNC) server allowed the radar modes to be changed by an off-side operator. VNC allowed access to the computer desktop leading up to control and change the radar modes to the ones convenient in the desired moment. These computers collected the data in these modes and the collected data was then accessed by either an ftp site or directly from the computers.

The S-band radar using VNC, was only allowed to communicate with the Communication Computer. The Radar Computer is configured to run the Profiler Online Program (POP) at start-up; this program is the one responsible of the actual data collection. POP writes hourly files allowing collecting as much data as desire as long the files hourly from the Radar Computer are moved to the Communication one using a batch file included in the computer desktop named “Move Files from Radar Computer”. The Radar Computer fills up in about two hours when running in “Precipitation Mode” so when the Radar Computer disk space is filled up the POP program continues running processing the profiles but the new data is not saved. The Communication Computer has two batch files icons on its desktop that allows switching from the “Normal Mode” to the “Precipitation Mode”. To verify which the last changed mode was, another icon for a batch file was added named “Last Changed Mode”. If the “Normal Mode” is the one working, the computer checks every hour by a routine for any mode changes. When the

radar is working under the “Precipitation Mode”, the computer checked for mode changes every 15 minutes. This is an important piece of information that has to be taken this into account at the time of running the radar in the desired mode. This way you know the exact amount of time you are collecting the data in this mode.

As previously mentioned, for the W-band radar, the Linux Machine communicates with the outside world. Thus, by using VNC it is allowed to access it and the others through it. To run the different parameters of the radar, several steps must be followed different from the S-band radar that has some batch files to be run. These steps directly control the radar working mode and collect data that is later recorded in the HP machine. The file is hourly closed and a new file is created. When the file is closed, it is moved from the HP machine to the Linux Computer and it is processed into time averaged netCDF format data and *gif* format images (see Figure3.4a for W band radar data and Figure 3.4b for S band radar data). This data is constantly monitored for quality control, usually the next day.

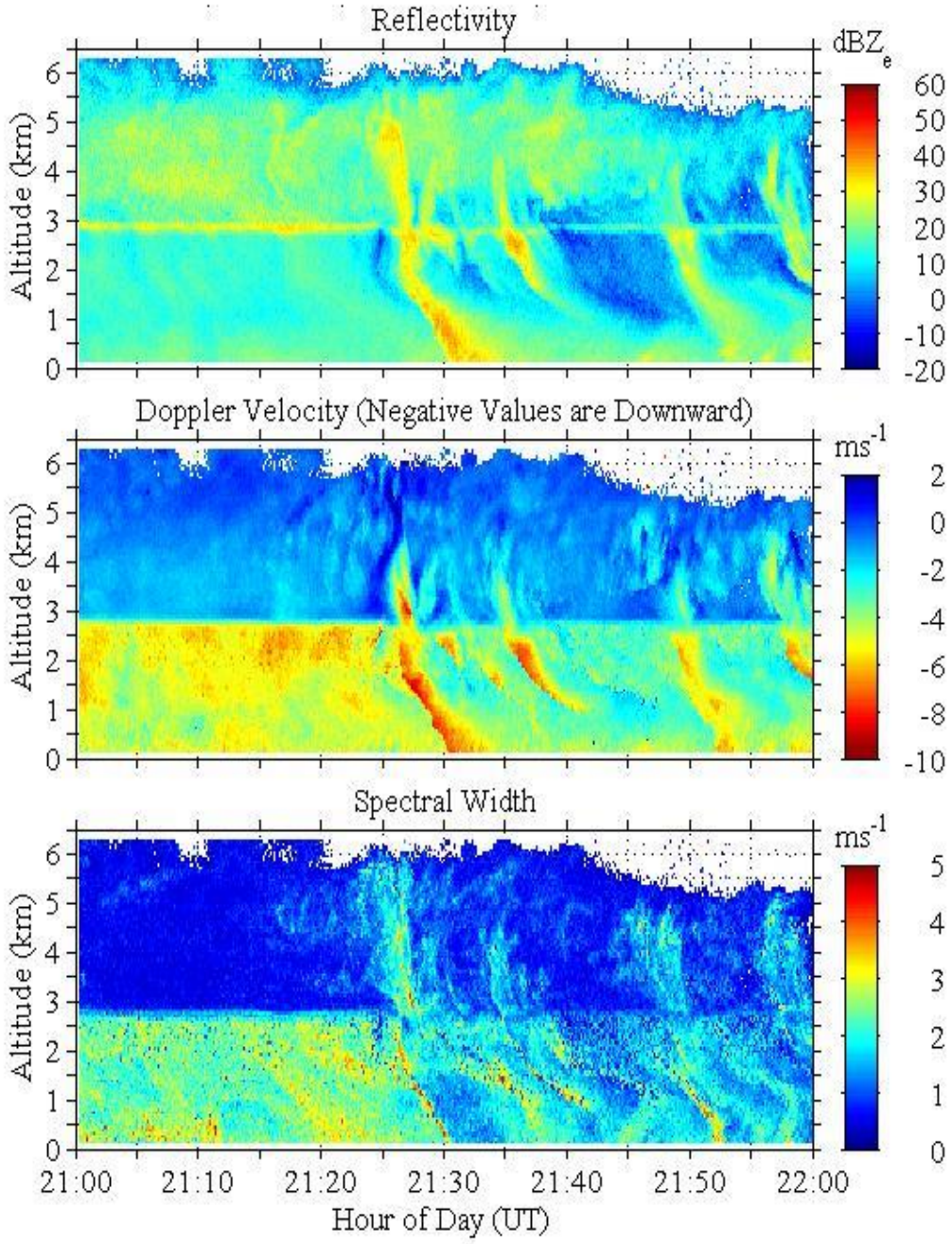

Figure 3.4a: S band radar collected data: Reflectivity, Doppler velocity, and Spectral width.

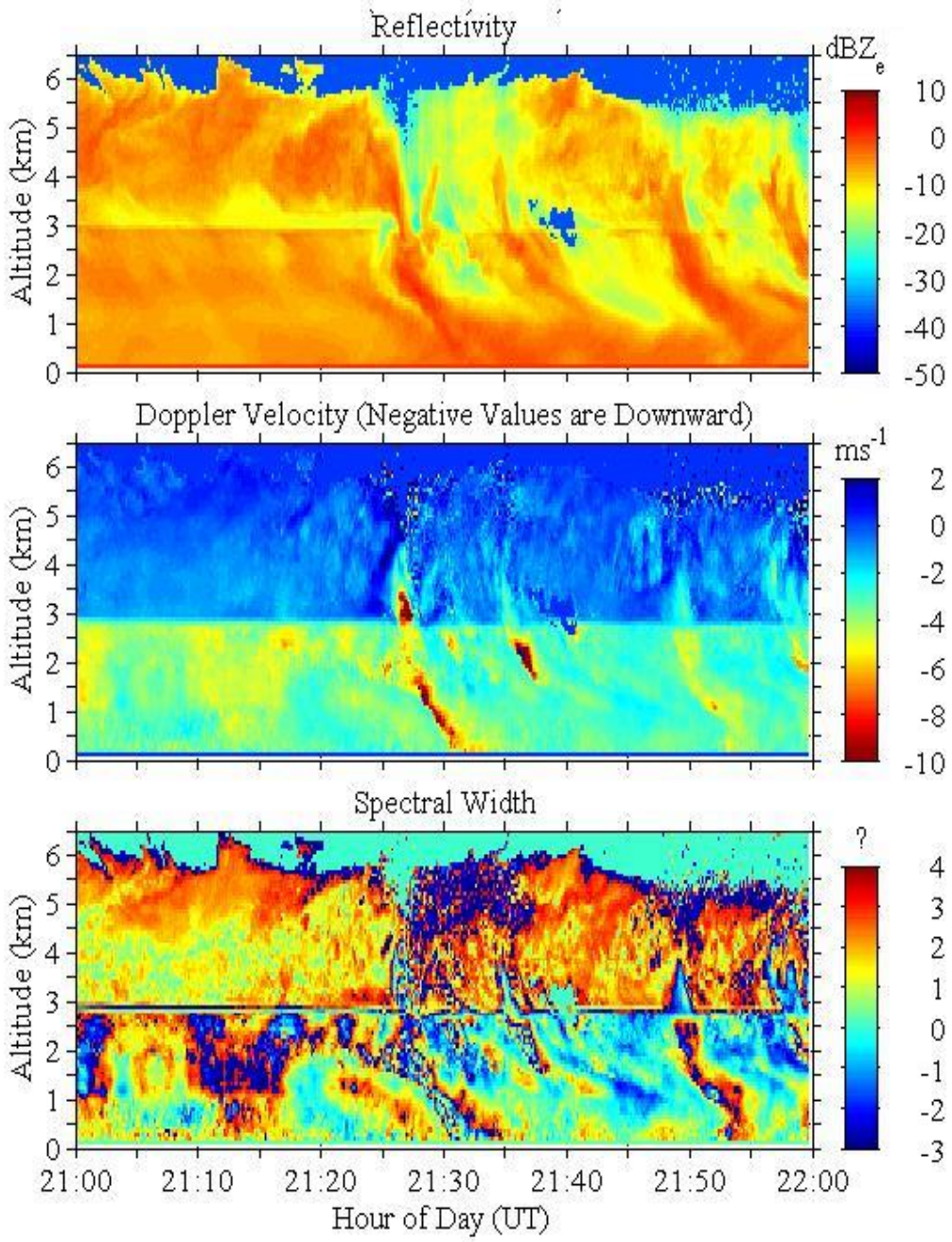

Figure 3.4b: W band radar collected data: Reflectivity, Doppler velocity, and Spectral width.

3.3 Data Processing

3.3.1 W-Band data Aliasing Removing and Data Alignment

The Doppler spectrum from the W-band radar exhibited velocity aliasing. This is shown in Figure 3.5 in which it can be seen that the spectrum wraps around to the positive values. The W-band spectra must be de-aliased in order to have correct values. A computer code was written for this purpose and is included in Appendix A.

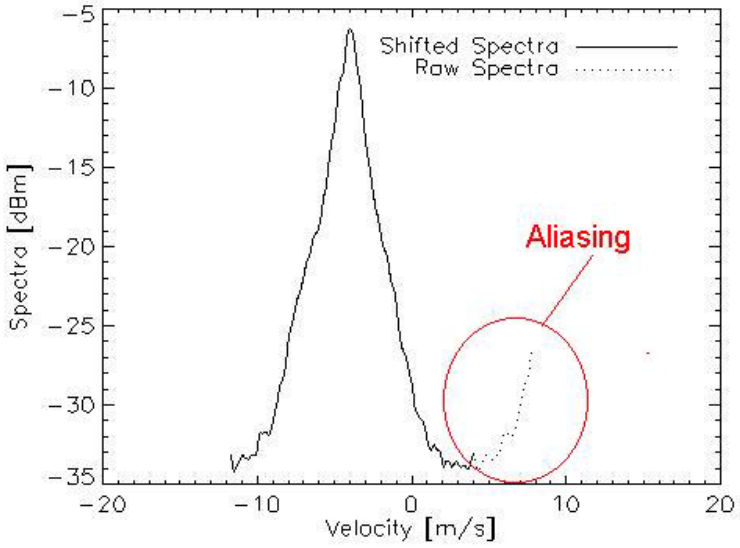

Figure 3.5: Doppler spectrum data from W-band radar showing aliasing. This case is for an altitude of 326.25 meters.

Another factor to consider is the data alignment. Both radars, even though they were near each other, were located at different places. Because of their different design, they also had different resolutions at the time setup for data collection. Their resolutions are described in Table 3.2.

Table 3.2: Description of the radars' and radiosonde data collection resolution.

Radar	Resolutions		
	Time [s]	Height [m]	Velocity [m/s]
W-band	10	75	0.123459
S-band	None	60	0.141464
Radiosonde	None	11	None

Therefore some common values had to be chosen to have the collected data in corresponding space, time and velocity bins. For hour 21:00:00 UTC start and end values of the data collected are described in Table 3.3. This table also shows the chosen values for the data alignment process.

Table 3.3: Start and end values of the collected data for hour 21:00 UTC and common values used to align data.

Radar	Time [s]		Height [m]		Velocity Axis [m/s]	
	start	*end*	*start*	*End*	*start*	*end*
W-band Radar	0	3,580	101.25	12,6026.3	-7.90140	7.77794
S-band Radar	17	3,599	114	6,294	-17.8245*	18.2489*
Radiosonde	none	none	315	22,183	none	none
Common Values	**17**	**3,557**	**114**	**6,084**	**-6.78125**	**7.10938**

*These values enclose 256 velocity bin points for which has to be reduced to 128 points as in the W-band data.

It can be observed in Table 3.3 that the radiosonde height start value is 315 meters. The common value of 114 meters was chosen in order that radar data was not lost. Because of this an extrapolation IDL code was developed to have RaOb data over the values from 114m and on. This code is presented in Apendix A.

Collected data was for up to 6km as seen in Figures 3.5a and 3.5b. In these figures, the melting layer can be distinguished at about 2.6 km; therefore, the data

considered for our purpose was restricted to be below the melting layer to ensure there are observed rain drops and not ice crystals. Reflectivity data for both radars used are shown in Figures 3.6a and 3.6b.

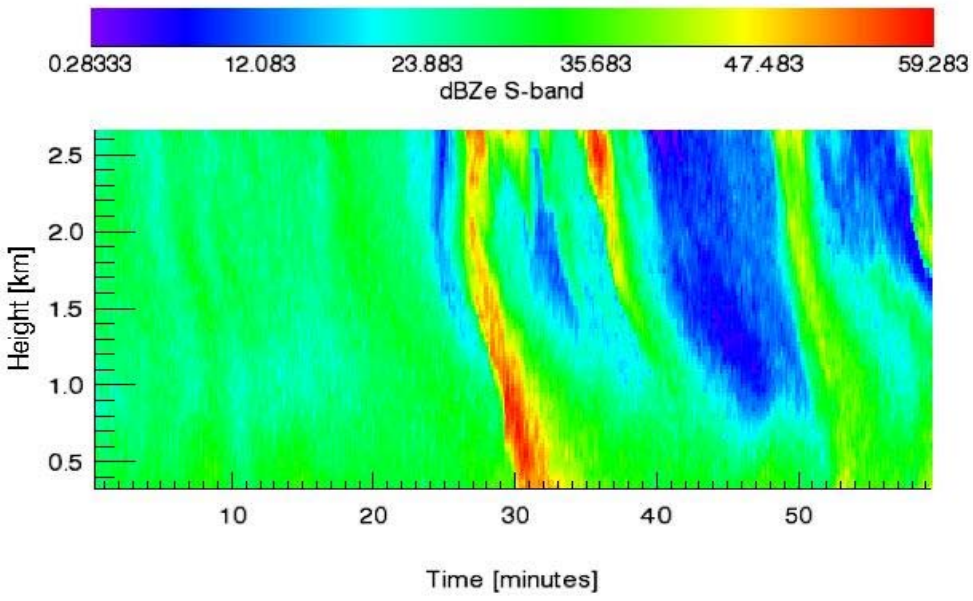

Figure 3.6a: Raw S-band Data below melting layer depicted in time and space.

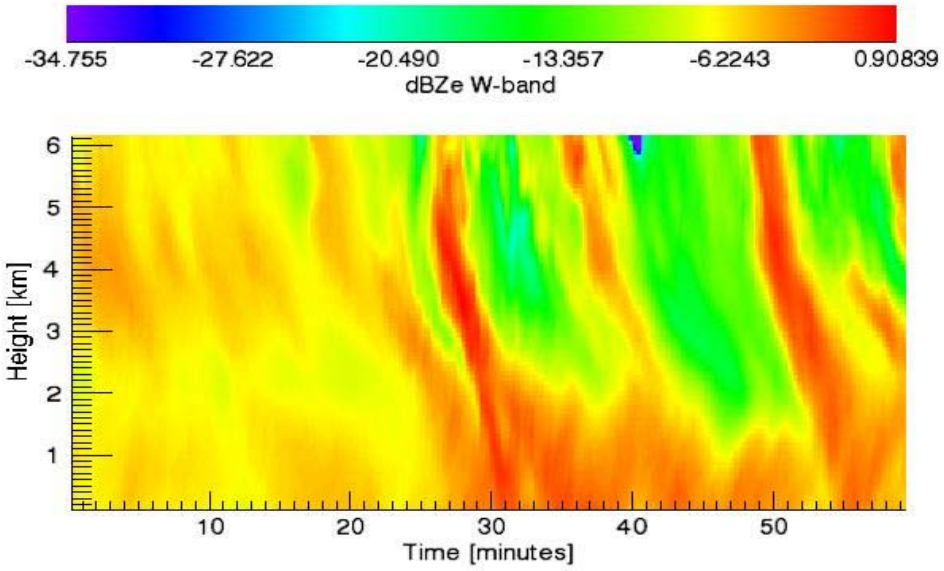

Figure 3.6b: Raw W-band Data below melting layer depicted in time and space.

From this data three different pixels were identified in order to show output values. The areas describe low, moderate and high rain activity, which reflectivity profiles are shown in Figures 3.7 through 3.9. Radar collected data for these areas are described in Table 3.4. These values are input to the codes as described further on in section 3.3.3.

Table 3.4: Measured values used for the data analysis.

Paramenters	**Region**	**Low**		**Moderate**		**High**	
	Radar	*S-band*	*W-band*	*S-band*	*W-band*	*S-band*	*W-band*
	dBZe	21.67	-4.62	27.53	-7.00	49.71	-0.73
	***v* [m/s]**	-6.01	-4.46	-5.69	-3.97	-7.12	-9.14
	Height	**1,.224 meters**		**804 meters**		**714 meters**	
	Time	**21:26:17 UTC**		**21:24:17 UTC**		**21:27:46 UTC**	

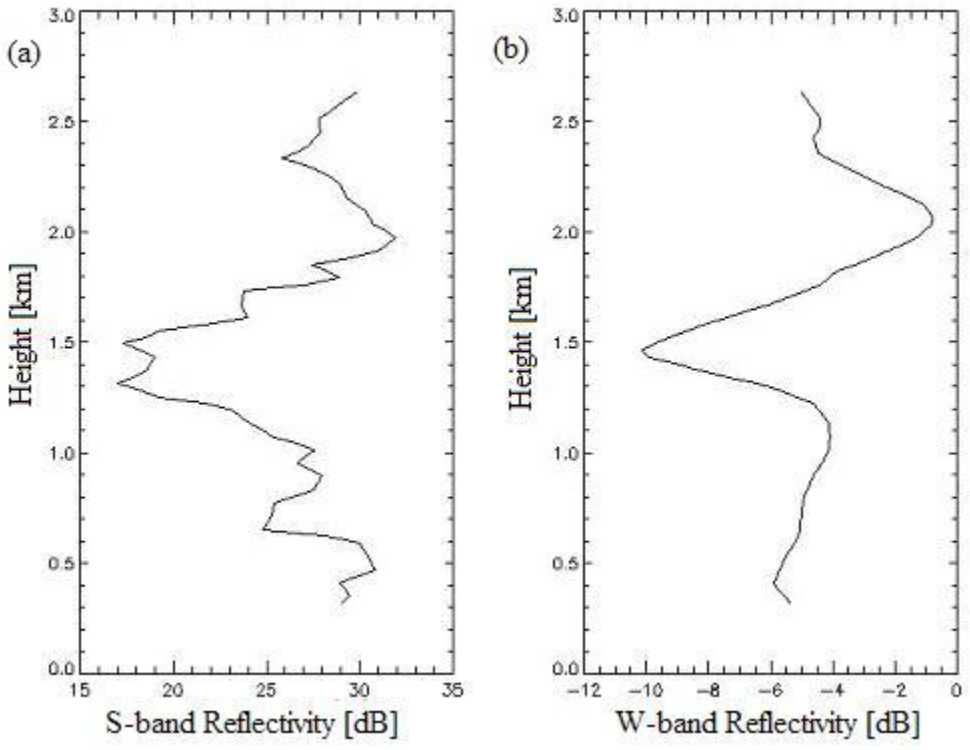

Figure 3.7: (a) S-band and (b) W-band reflectivity profile for the cell at 21:26:17 UTC

minutes and 1.224 km height.

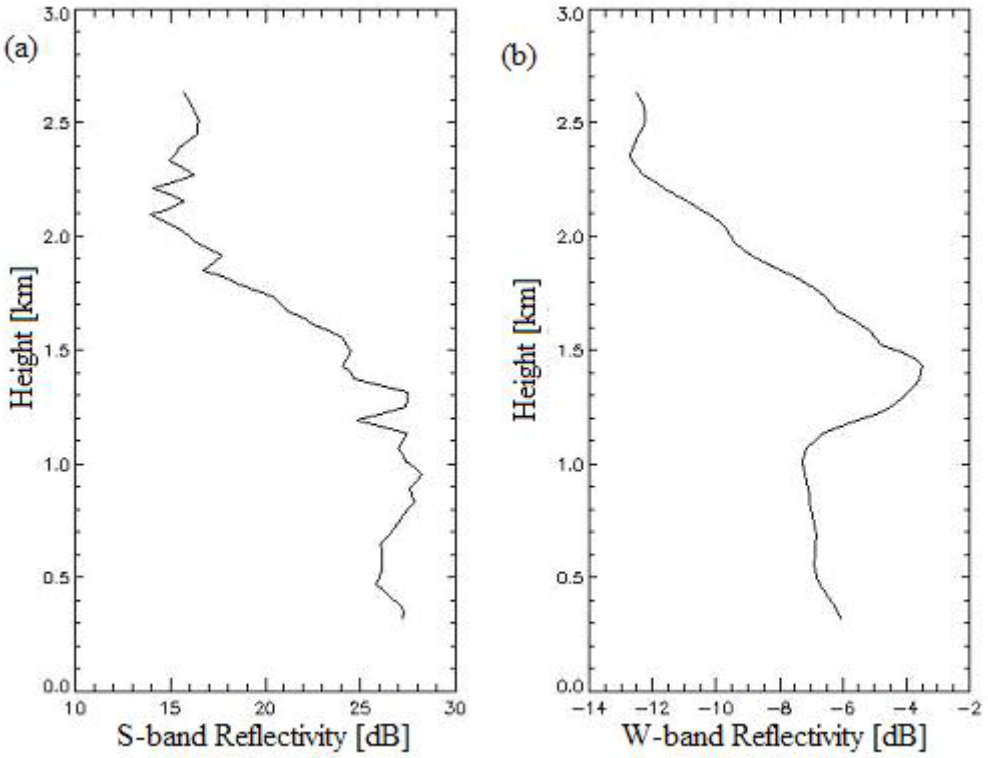

Figure 3.8: (a) S-band and (b) W-band reflectivity profile for the cell at 21:24:17 UTC minutes and 804 meters height.

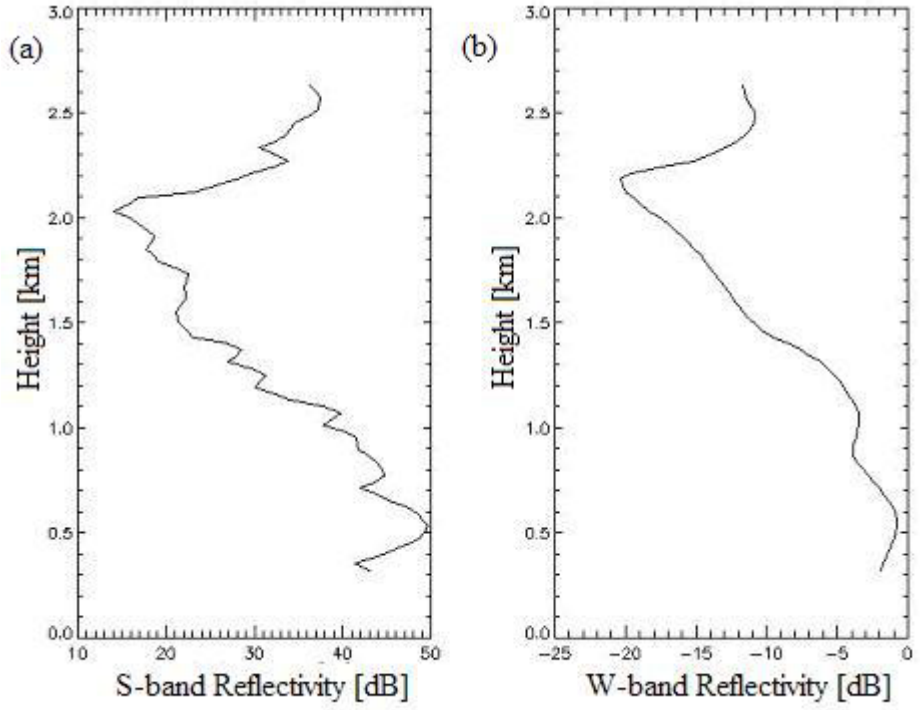

Figure 3.9: (a) S-band and (b) W-band reflectivity profile for the cell at 21:27:46 UTC minutes and 714 meters height.

3.3.2 Radiosonde and Liebe Model's Parameters

Radiosonde parameters profiles were retrieved for up to 12km but the data considered was below melting layer located at 2.6km. Figure 3.10 shows temperature and pressure profiles for up to 6km height.

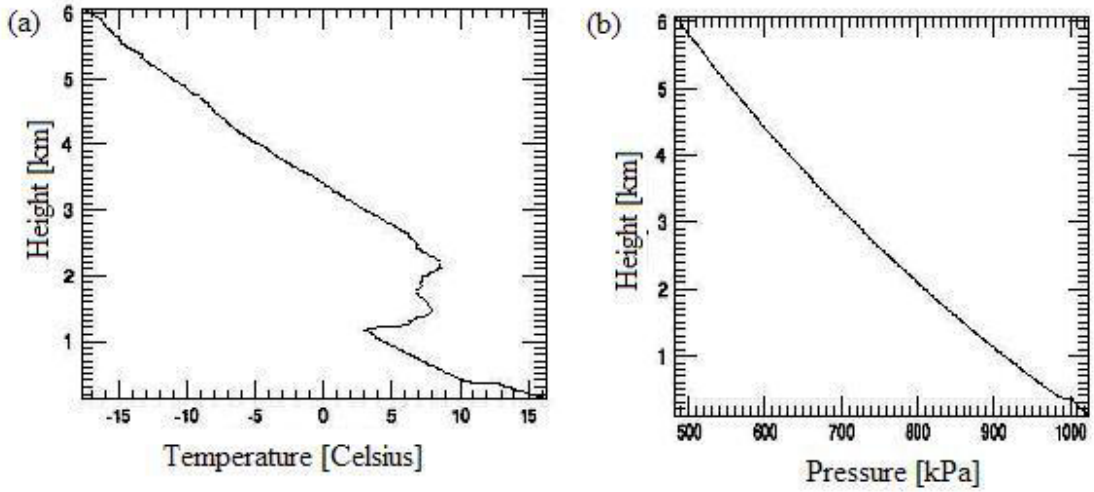

Figure 3.10: (a) Temperature profile provided by the radiosonde observations. (b) Pressure profile provided by the radiosonde observations.

As described in section 3.1.3, these temperatures are used to calculate the refractive index (see Figure 3.11) at each layer and both, the pressures and temperatures, are used to compute the air desity correction factor (see Figure 3.12).

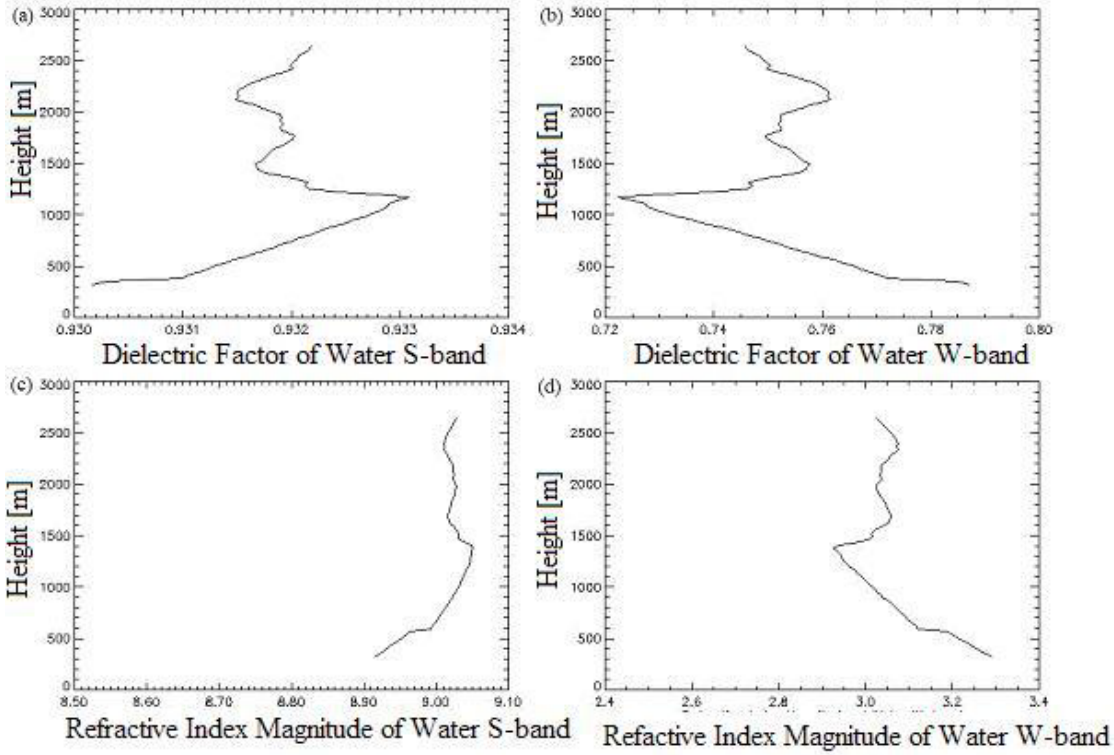

Figure 3.11: Liebe's model for water droplets parameters of Dielectric Factor (a) S-band and (b) W-band and Refractive Index magnitude of water (c) S-band and (d) W-band vs. Height.

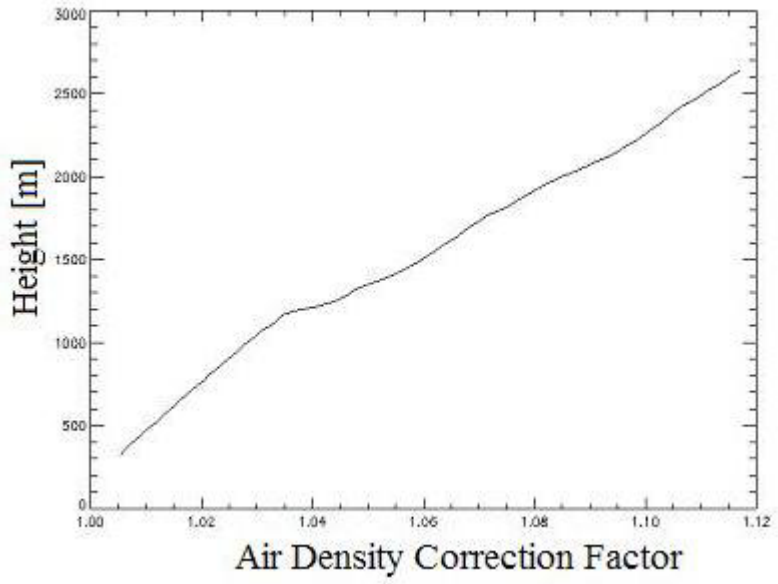

Figure 3.12: Air Density correction factor used to correct droplets velocities.

3.3.3 Dual Frequency Method

The proposed data analysis (based upon Firda's work) [*Firda et al.*, 1999, *Firda* 1997] starts from a single range cell with simulated values and moving up to the next higher cell until the whole profile is done and then it moves up to the next time profile The flow diagram is shown in Figure 3.13 in a general way. It consists of 2 steps, the rainfall rate retrieval for the first cell, and the vertical air motion effect removal.

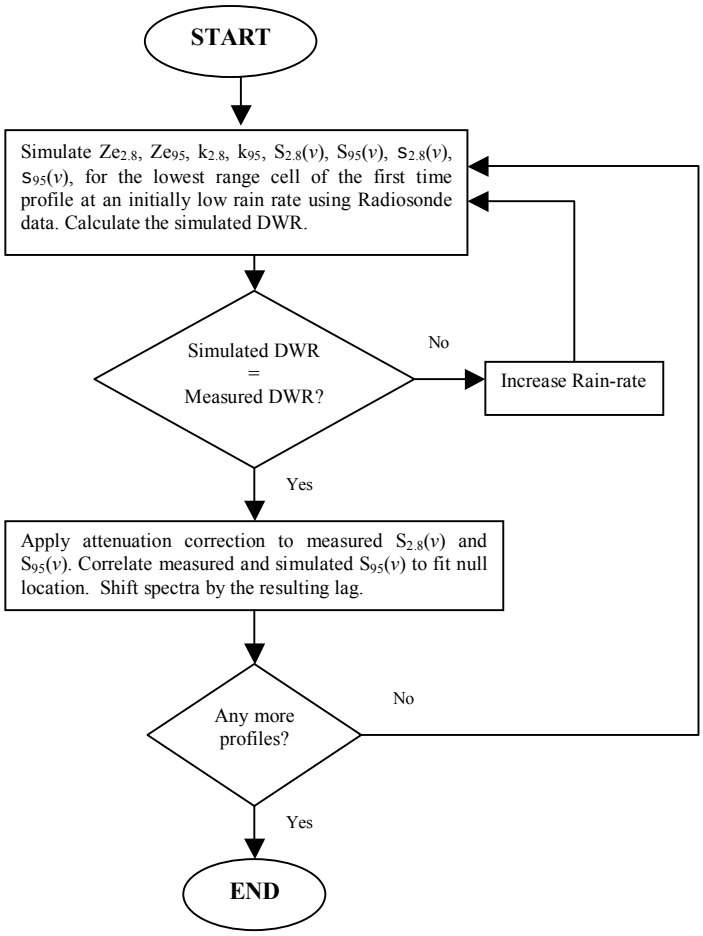

Figure 3.13: Flow diagram for the iterative method to be followed for data processing.

3.3.3.1 Rainfall Rate Retrieval

Located at the very first time and range cell, temperature's radiosonde data is used as input to Liebe's model for suspended water droplets to calculate the complex refraction index n_w and the dielectric factor $|K_w|^2$, at both 2.8 and 95 GHz. These values are used to simulate the backscattering and extiction crossections used to simulate the spectrum, attenuation and reflectivity (see equations 13, 32, and 34 respectively) (see

Figure 14). With these values the simulated *DWR* is calculated following equation 37 with the obtained simulated reflectivities. This value is compared to the measured one for that cell (see Figure 3.14).

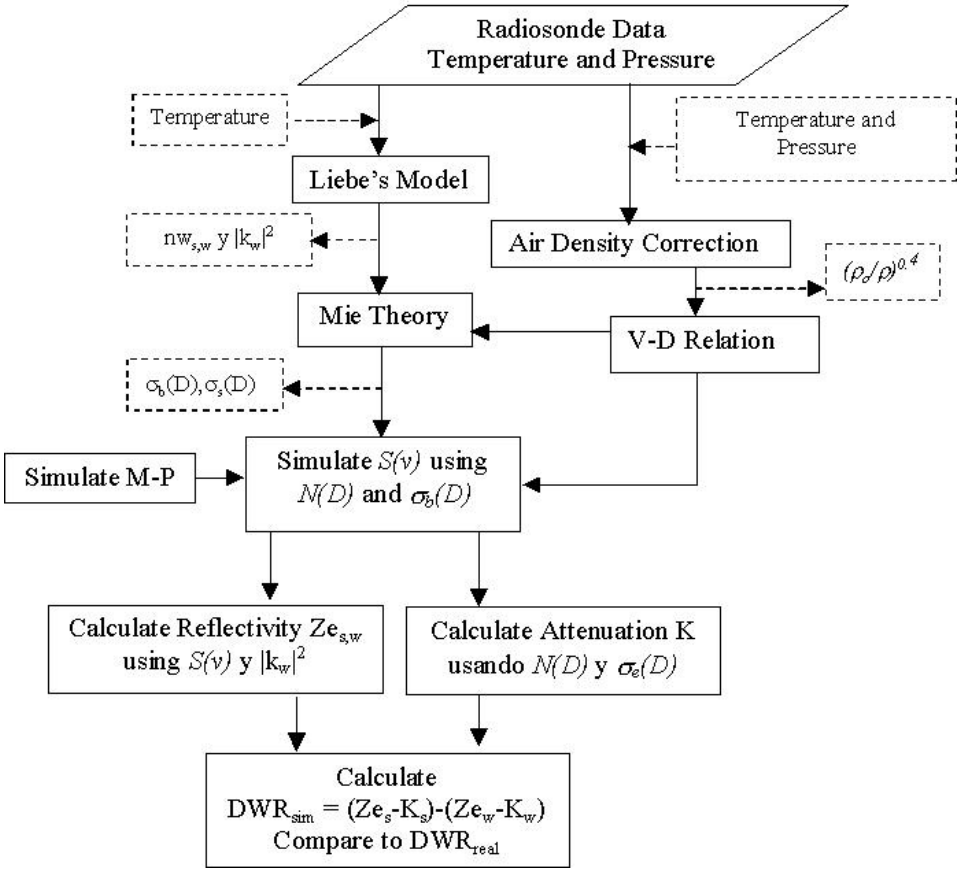

Figure 3.14: Flowchart explaining the rainrate retrieval for the all range cell.

In $S(v) = N(D)\sigma_b(D)(dD/dv)$ is composed of three parts, the drop-size distribution, the backscattered crossection, and the velocity-diameter relation. If the simulated DWR is not equal to the measured one, the rain-rate is increased in equation 25, and compared DWRs again. This is done until until both quantities are the same indicating the real rain-rate.

3.3.3.2 Vertical Air Motion

With the obtained rain-rate, the spectra and attenuation for that cell are simulated and compared to the measured spectra for that cell. To extract the vertical air motion, the velocity axis is moved until the first nulls of the measured and simulated spectra correlates as explained in section 2.2.6.1.

CHAPTER 4

RESULTS

4.1 Low, Moderate and High rain rate pixels analysis

The three different pixels considered in the analysis, described in section 3.3.1 represent low, moderate and high rain activity. The method described in section 3.3.3.2 to retrieve the rainfall rate used the simulated backscattering coefficient shown in Figure 4.1 to analyze the low rain activity pixel, located at 21:26:17 UTC and 1.224 km height. The returned the values of attenuation, *DWR*, reflectivity, mean velocity and differential velocity are described in Figures 4.2 a, through e. These cell values show a rain-rate of 4.88 mm/hr.

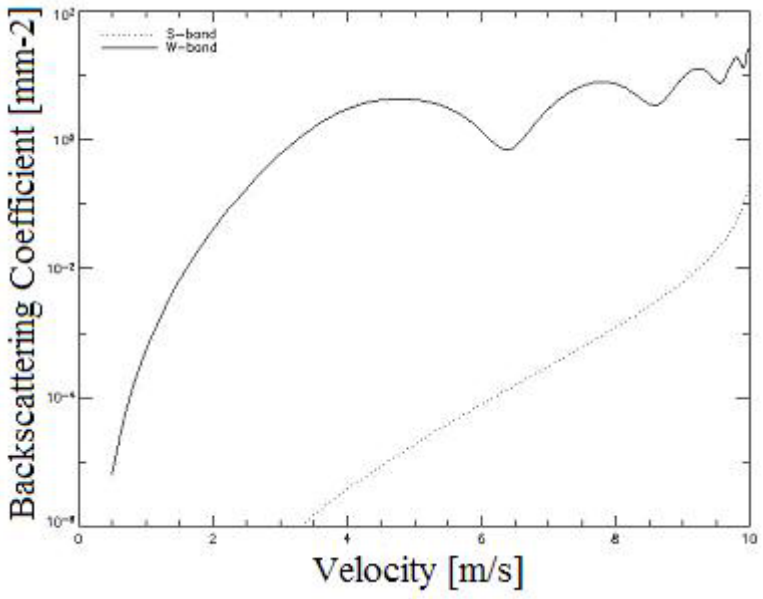

Figure 4.1: Backscattering coefficient for both radar frequencies for the low rain rate pixel.

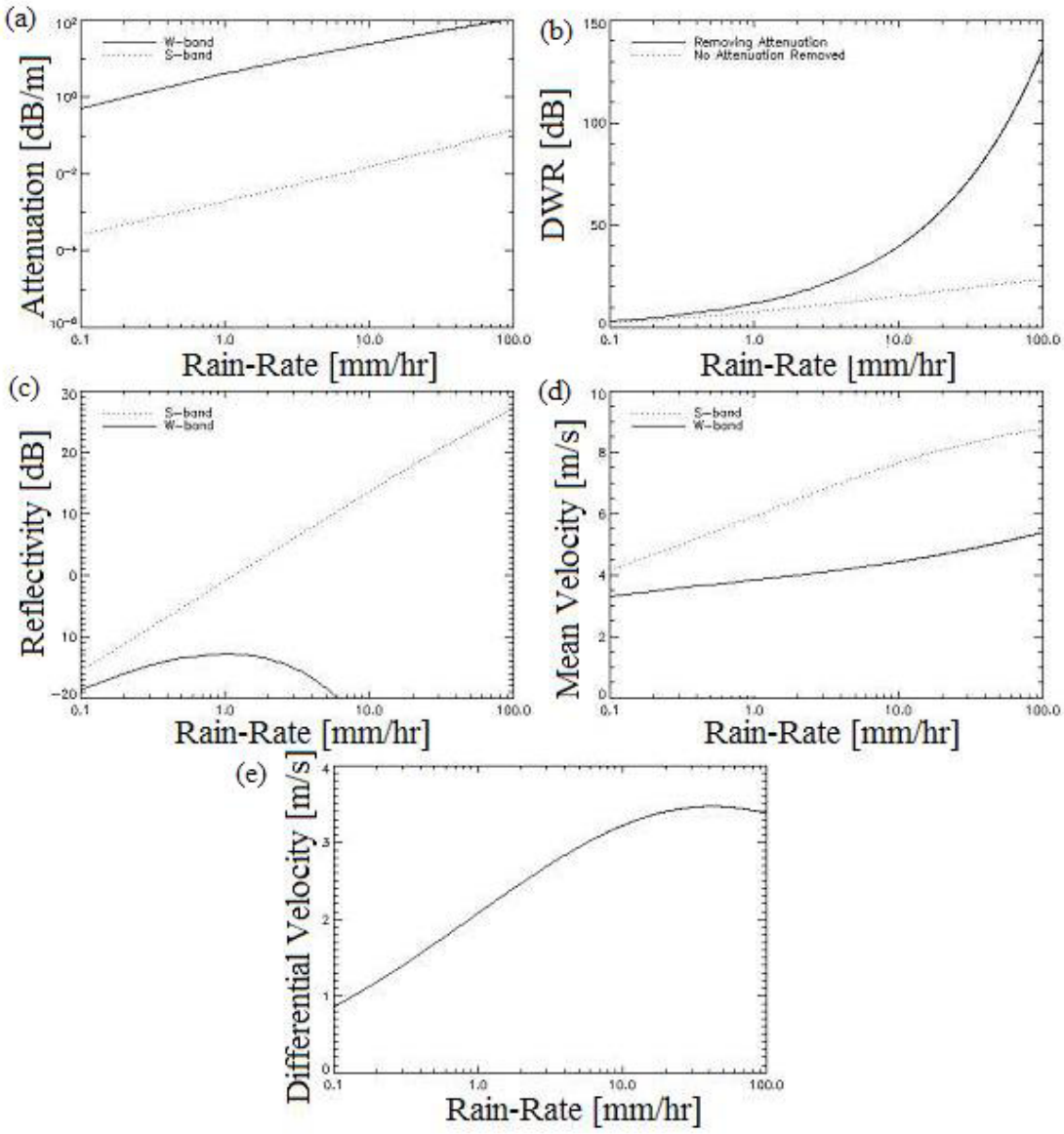

Figure 4.2: (a) Attenuation, (b) DWR, (c) Reflectivity, (d) Mean Velocity, and (e) Differential velocity simulated values vs. Rain Rate for the profile cell at 21:26:17 UTC minutes and 1.224 km height.

Using this value, the spectra was simulated and compared to the measured spectra to locate the first null and retrieve the vertical air motion. This comparison resulted in a

vertical air motion of 2.33 m/s. The measured spectrum bias is shown in Figure 4.3. Figure 4.4 shows the simulated and measured spectra for this cell.

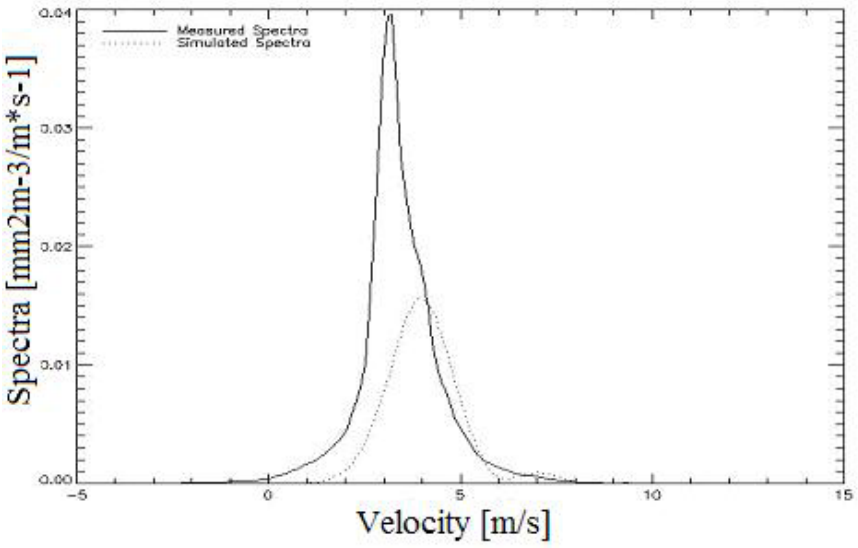

Figure 4.3: Shifted and non shifted measured spectra by the vertical air motion in cell at 21:26:17 UTC minutes and 1.224 km height (Low rain activity cell).

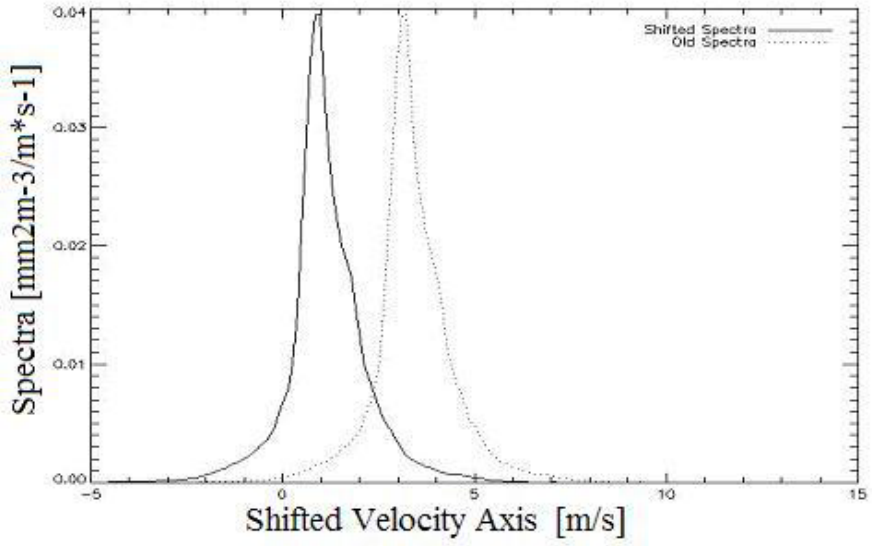

Figure 4.4: Simulated and Measured spectra used to retrieve the vertical air motion in cell at 21:26:17 UTC minutes and 1.224 km height.

A moderate rain activity area was located at time 21:24:17 UTC and 804 meters height. The backscattering coefficient used in the processing is shown in Figure 4.5. Using these coefficients, the values returned from the code are depicted in Figure 4.6 a, b, c, d, and e.

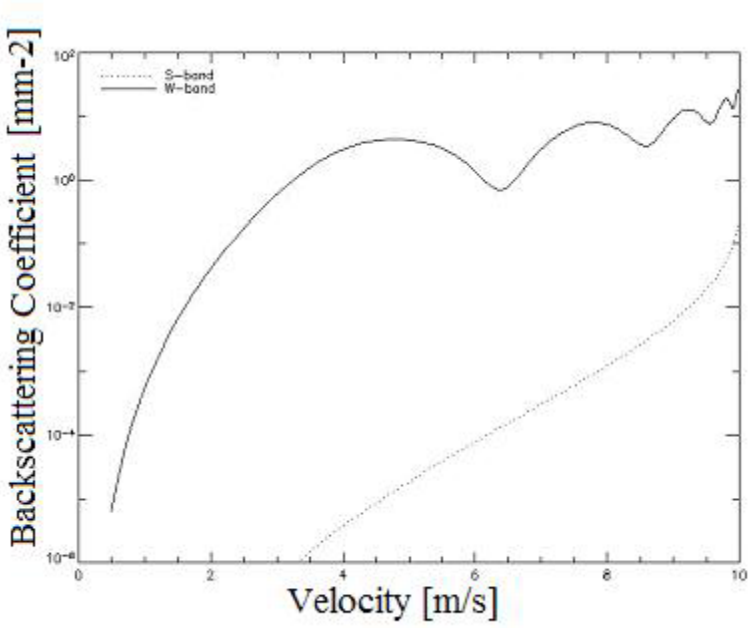

Figure 4.5: Backscattering coefficient for both radar frequencies for the moderate rain rate pixel.

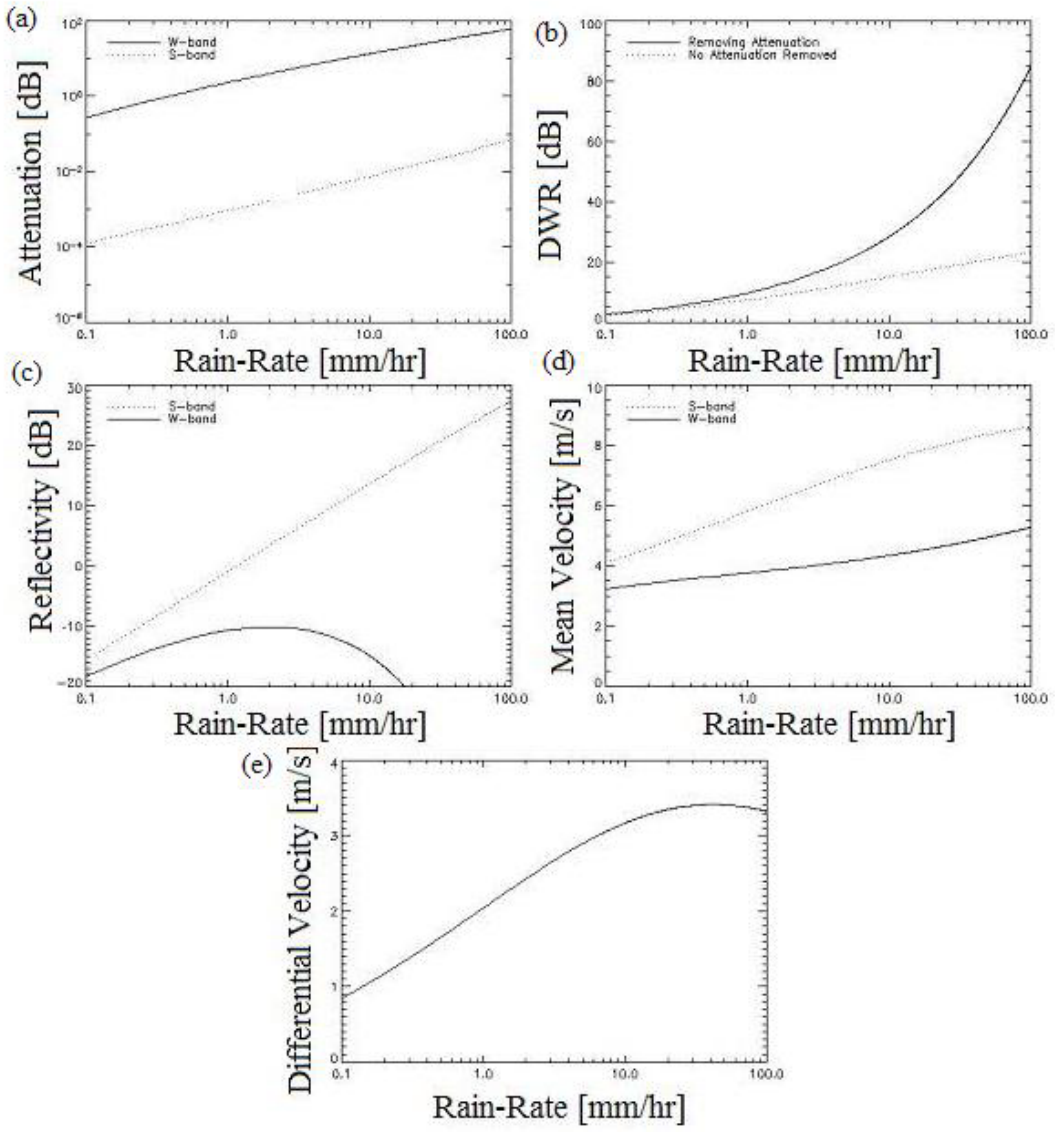

Figure 4.6: (a) Attenuation, (b) DWR, (c) Reflectivity, (d) Mean Velocity, and (e) Differential velocity simulated values vs. Rain Rate for the profile cell at 21:24:17 UTC minutes and 804 meters height.

The rainfall rate for this cell was 16.4 mm/hr. This value was used to simulate the W-band spectra and retrieve a vertical air motion of 2.11 m/s found on this cell. The spectrum shifting caused by this vertical air motion is shown in Figure 4.7. The simulated and measured spectra are shown in Figure 4.8.

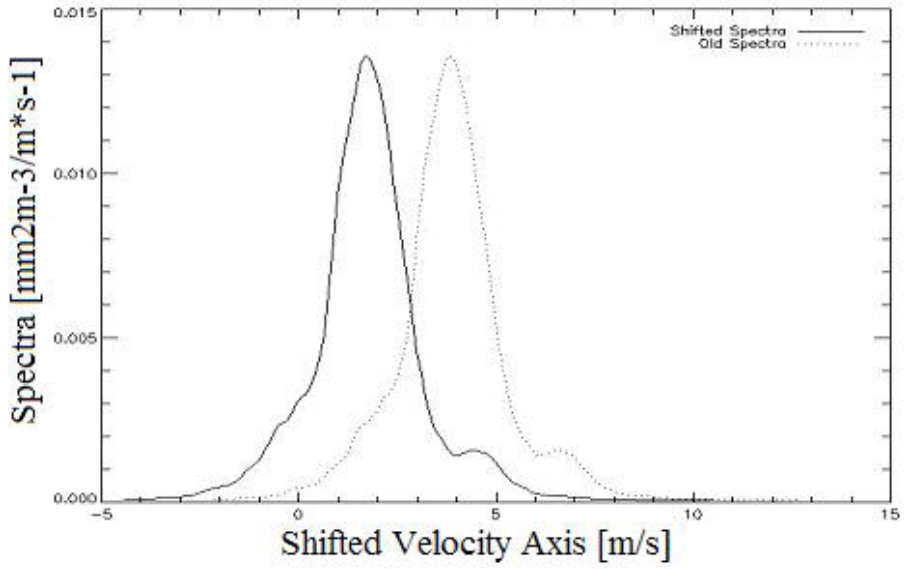

Figure 4.7: Shifted and non shifted measured spectra by the vertical air motion in cell at 21:24:17 UTC minutes and 804 meters height (Moderate rain activity cell).

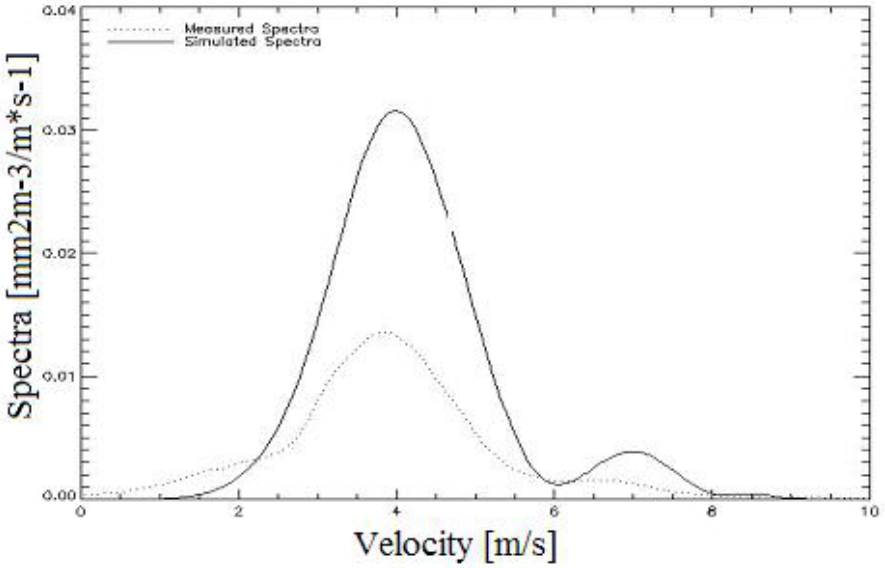

Figure 4.8: Simulated and Measured spectra used to retrieve the vertical air motion at 21:24:17 UTC and 804 meters height.

Similarly, the high rain fall activity area, located at 21:27:46 UTC and 714 meters height, used the backscattering coefficient shown in Figure 4.9. The code returned the values shown in Figure 4.10. A rain-rate of 43.98 mm/hr was found.

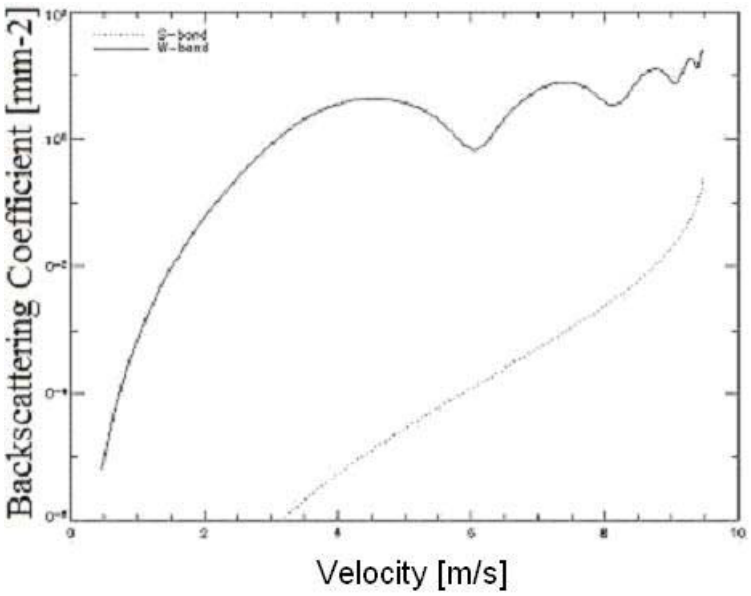

Figure 4.9: Backscattering coefficient for both radar frequencies for the high rain rate pixel.

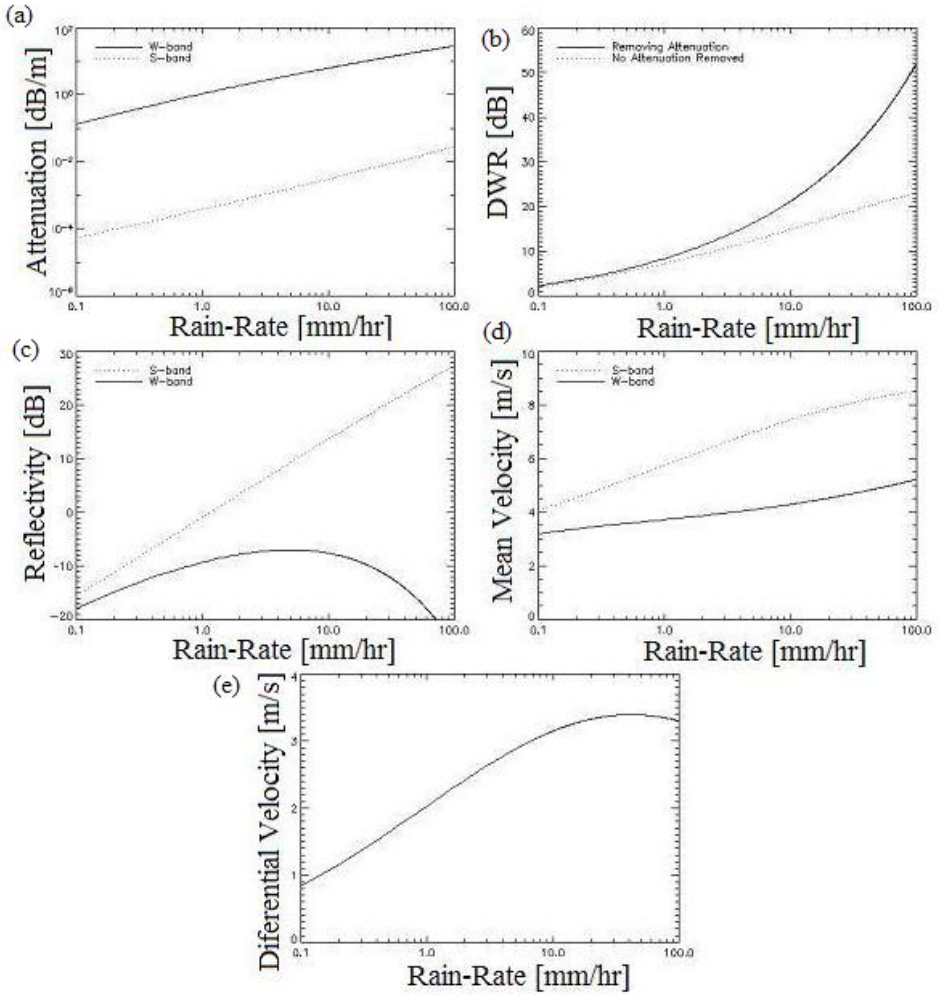

Figure 4.10: (a) Attenuation, (b) DWR, (c) Reflectivity, (d) Mean Velocity, and (e) Differential velocity simulated values vs. Rain Rate for the profile cell at 21:27:46 UTC minutes and 714 meters height.

The shifting in the velocity axis is shown in Figure 4.11 where an downdraft of 2.01m/s was retrieved. The simulated and measured spectra shown in Figure 4.12 were used to retrieve the vertical air motion. Table 4.1 summarizes the values described previously.

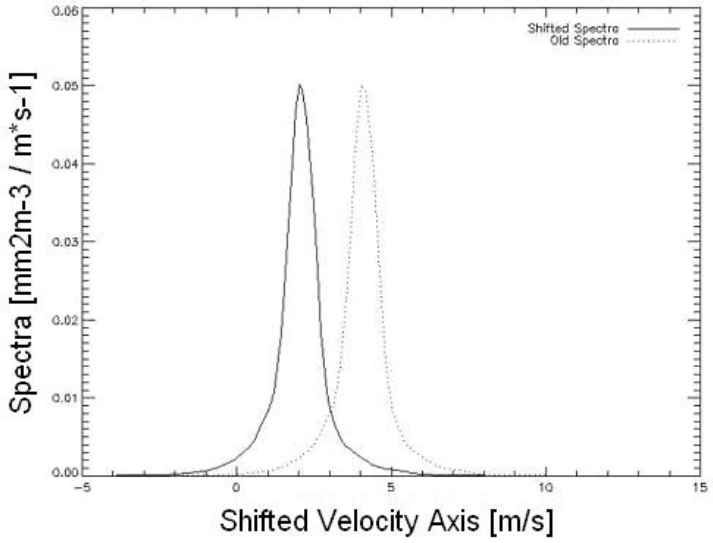

Figure 4.11: Shifted and non shifted measured spectra by the vertical air motion in cell at 21:27:46 UTC minutes and 714 meters height (Low rain activity cell).

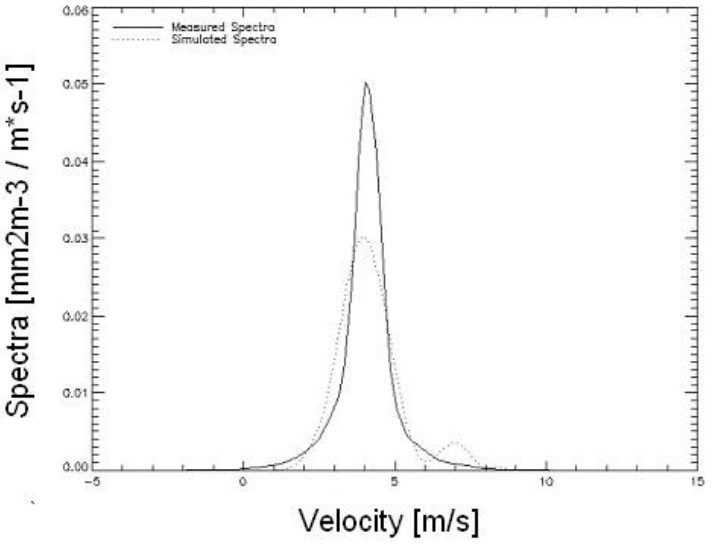

Figure 4.12: Simulated and Measured spectra used to retrieve the vertical air motion at 21:27:46 UTC and 714 meters height.

Table 4.1: Values found for the three different rain activity areas.

	Low	**Moderate**	**High**
Rain-Rate [mm/hr]	4.88	16.4	43.98
Vertical air motion [m/s]	2.33	2.10	2.01

Rain rate was retrieved from the processed data. A sample area of data (shown squared in Figure 4.13), where the three cases pixels were selected, is shown in Figure 4.14. This figure shows the retrieve rain rates for all the different pixels from time 21:17:07 UTC through 21:33:37 UTC.

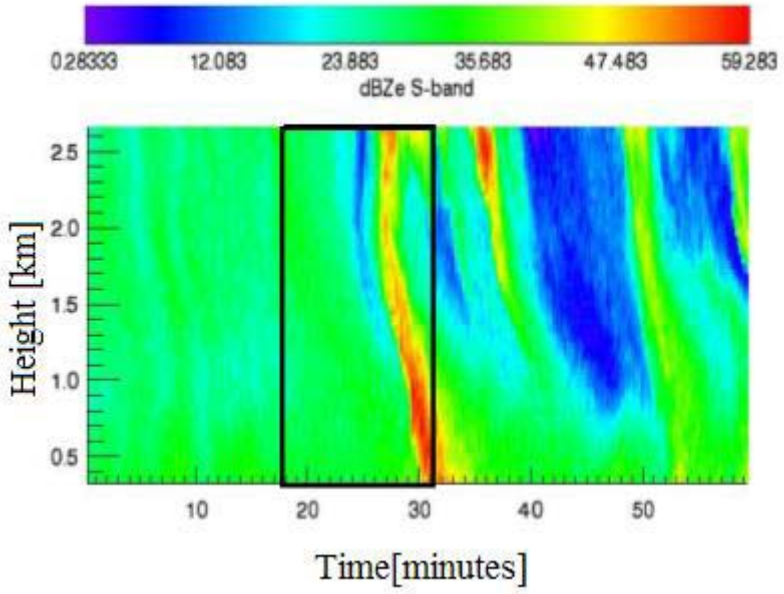

Figure 4.13: Selected area from which the low, moderate and hight rain rate pixels were chosen.

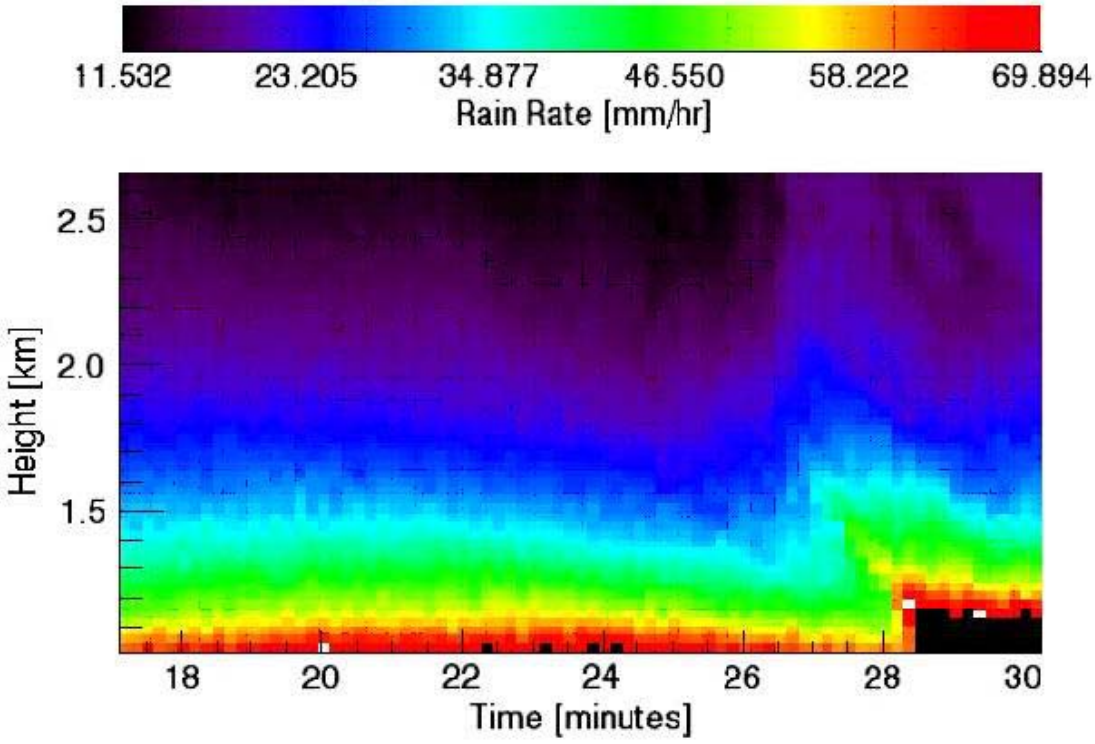

Figure 4.14: Rain rate retrieved in time and space starting at 21:17:07 UTC and ending at 21:33:37 UTC.

For this region the vertical air motion was also retrieved. Their values are depicted in Figure 4.15 which shows that vertical air motion region ranges between downdrafts of -1.2 to updrafts of 2.5 m/s.

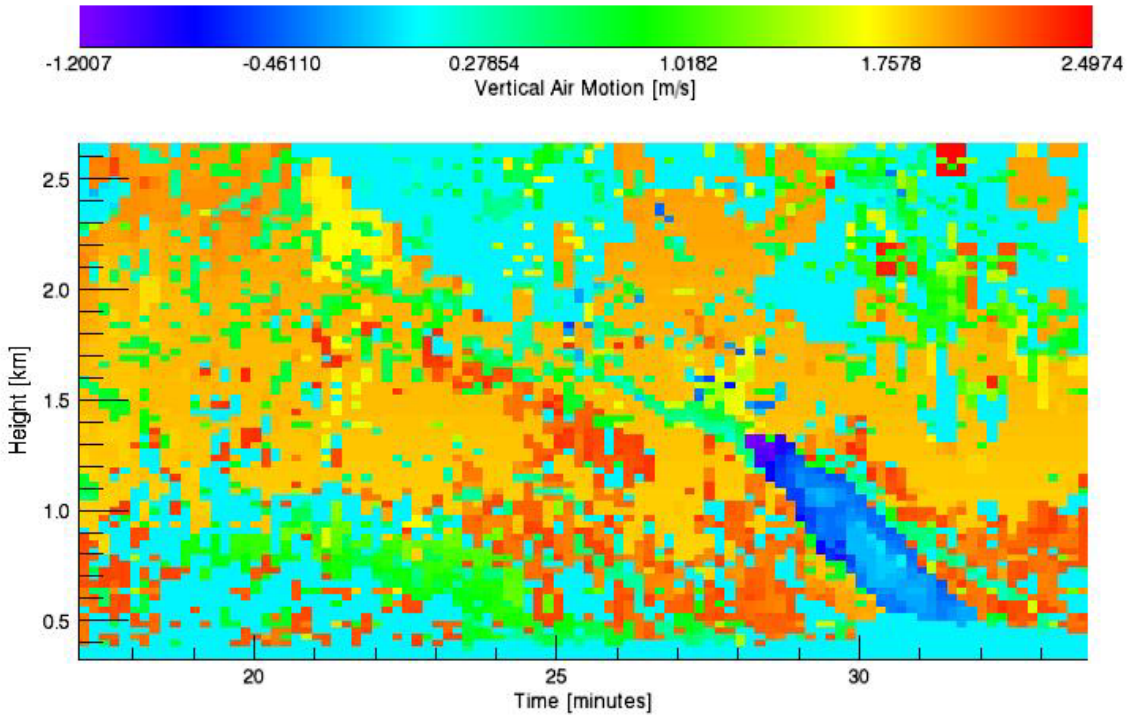

Figure 4.15: Vertical air motion retrieved, from time 21:17:07 to 21:33:37 UTC, depicted in time and space.

CHAPTER 5

CONCLUSIONS AND FUTURE WORK

Accurate rainfall rates and vertical air motion are of vital importance in retrieving drop size distribution in rain. Therefore the challenges included retrieving accurate results from the used algorithms, which in our case assume a Marshall-Palmer drop size distribution, and removing attenuation from simulated values.

The dual-frequency method used to retrieve the rain rates and vertical air motion demonstrated its ability to estimate these parameters. Some cells exhibited a W-band equivalent under -35dB which corresponds to no rain activity and therefore no vertical air motion could be estimated. In this case both quantities were set to zero.

In Figure 3.6, the area between 21:30:00 UTC and 21:35:00 UTC shows a high rain activity area which is reflected in the vertical air motion and rainfall rates retrievals. Reflectivities from S-band and W-band show their highest values around this area, so do rain rates and vertical air motion.

Figures 4.2b. 4.6b, and 4.10b show the dual wavelength ratio with and without the attenuation removed. This shows the base impact of the attenuation on the radars' signal and the way it affects the rain rates retrieval. For example, in the moderate rain activity case, reflectivities of 27.53dB and -7dB show a DWR of 34.53dB, which clearly marks a difference between the real rainfall rate (in this case would be around 16 mm/hr) and the

one without the attenuation removed (is has higher than 100 mm/hr). This indicates that the algorithm is underestimating the actual rainfall rate. The dual frequency method used here and described in section 3.3.3 takes this attenuation removal into account.

Rainfall rates were retrieved for the data analyzed. Vertical air motion was also retrieved and removed from the measured spectra. These estimates were based upon assuming a Marshall-Palmer raindrop size distribution. This assumption would lead to uncertainties in the rainfall rate retrieval due to differences between real distribution and the Marshall-Palmer, whose model better describes the raindrop size distribution within the cells. Therefore these outputs would serve as inputs to a code which can calculate the real drop size distribution. Only vertical air motion was removed from data but turbulence also affects the distribution, therefore must be removed.

This algorithm is not accurate for hail since the models used considers only rain. A hail event can be observed at hour 21:30:00 UTC as a streak starting from around 3 km height. This algorithm can be improved by adding a routine to correct for hail presence.

Models often require a set of validation experiments to examine its performance over the range of parameters to be estimated. Because of the uncertainties with respect to the real rainfall rates retrieved, we expect there to be differences between experimental observations and the model predictions. Therefore validation experiments are of vital importance since they take into account measurements and model uncertainties. It is

recommended to develop a validation experiment in order to prove the efficiency of this model. This can be done using another data set, with the same frequencies used in this experiment, as inputs to the model, and in-situ rain gauges measurements, or disdrometer data as ground-truth values to compare with our results.

REFERENCES

Doviak, Richard J., Zrnić, Dušan S., *Doppler Radars and Weather Observations*, Academic Press, Second Edition, 1993.

Firda John M., "Application of Dual-Frequency Millimeter-Wave Doppler Spectra for the Retrieval of Drop Size Distributions and Vertical Air Motion in Rain", *Dissertation*, September 1997.

Firda, John M., "Application of Dual-Frequency Millimeter-Wave Doppler Spectra for the Retrieval of Drop Size Distributions and Vertical Air Motion in Rain", *Journal of Atmospheric and Oceanic Technology*, Vol. 16, pp.216-236, 1999.

Green A. W., *"*An Approximation for the Shapes of Large Raindrops*"*, *Journal of Applied Meteorology,* Vol. 14, pp.1578-1583, 1975.

Gunn, R., G.D. Kinzer, "The terminal velocity of fall for water droplets in stagnant air.", J.Meteor., **6**, pp.243-248, 1949.

Hogan, R. J., A. J. Illingworth, and H. Sauvageot, "Measuring crystal size in cirrus using 35- and 94-GHz radars", *Journal of Atmospheric and Oceanic Technology*, Vol. 17, pp.27-37, 2000.

Lhermitte, R., "Observations of rain at vertical incidence with a 94GHz Doppler Radar: An insight on Mie Scattering", *Geophysical Research Letters*, Vol. 15, pp.1125-1128, 1988.

Liebe, H. J., 1989: MPM-An Atmospheric Millimeter-Wave Propagation Model. International *Journal of Infrared and Millimeter Waves*, **10**, no. 6

Lutgens, F. K., and E. L. Tarbuck, 1998: *The Atmosphere*. Chapter 5, Seventh Edition, Prentice Hall.

Marshall, J.S., Palmer, W.M., "The distribution of raindrops with size", *Journal of Meteorology*, Volume 5, pp.165-166, 1948.

Rincón Rafael F., Lang Roger H., "Microwave Link Dual-Wavelength Measurements of Path-Average Attenuation for the Estimation of Drop Size Distribution and Rainfall", *IEEE Trans. Geoscience and Remote Sensing*, Vol. 40, No. 4, pp.760-770, April 2002

Rogers, R.R. and Yau, M.K., *A Short Course in Cloud Physics*, Third Edition, Butterworth-Heinemann Publications.

Sauvageot, Henri, *Radar Meteorology*, Artech House, Inc.,1992

Ulaby, F. T., Moore R. K., Fung A. K., *Microwave Remote Sensing*, Addison Wesley, Volume 1, Chapter 5, 1986.

APPENDICES: IDL PROGRAMS

Programs

Programs used to retrieve, and align Radiosonde data

```
        ;PROGRAM THAT READS AND SAVE RaOb data after extrapolating range array
        ;Enero/30/2003
        ;Leyda Leon - RUM

        ;This program starts RaOb cells over 1km height...

        ;READING RaOb FILE

        restore, filename="C:\My Documents\LeydaUPRM\Rain\2003\RaOb\RaObraw.dat" ;RESTORES
RAOB RAW DATA

        ;Get RaOb needed data from the whole RaOb Array

        extrapol, pres, tair, rh, alt, AltR, TairR, PresR, RhR

        ;Collocate data with Radars data

        raobcollocate, AltR, TairR, PresR, RhR, range_fixed

        ;###############################################################################
####################
        ;SAVING ALL VARIABLES INTO .DAT FILE


        SAVE , timeRaOb, latR,lonR, TairR, PresR, RhR, range_fixed,$
                FILENAME  =  "C:\My  Documents\LeydaUPRM\Rain\2003\Data2003\RaOb_2003.dat"
;saving the variables...


End

        ;Program that extrapolates RaOb data to rangeS
        ;January 30, 2003
        ;Leyda Leon - RUM


        PRO extrapol, pres, tair, rh, alt, AltR, TairR, PresR, RhR

        tair1=tair
        ;window,0
        ;plot,  tair,  alt,  yrange  =  [0,1000],xtitle="Temperature  Raw  RaOb  Data  [C]",
ytitle="Height [m]"


        hmax = max(alt)
        hmin = min(alt)

        rfixmax = 6084 ;para que llegue hasta el 6049 y luego interpolar en menos
        rfixmin =114

        mh = (alt(3)- alt(0)) / 3
        mt  = (tair(3)-tair(0)) / 3
        mp =  (pres(13)-pres(0)) / 13
        mrh = (rh(13)-rh(0)) / 13

        ;EXTRAPOLATION
        ;Definiendo los limites

        lup = 19.
```

```
ldown = 0.

;Definiendo los arreglos
h = fltarr(lup)
t = fltarr(lup)
p = fltarr(lup)
relh = fltarr(lup)

FOR y = ldown, lup-1 DO BEGIN

  h(y) = y * mh + rfixmin
  if h(y) gt alt(0) then goto, jumpout1

ENDFOR

jumpout1:

b_tairR = tair(0) - mt * lup
FOR y = ldown, lup-1 DO BEGIN
  t(y) = y * mt +  b_tairR
ENDFOR

b_presR = pres(0) - mp * lup
FOR y = ldown, lup-1 DO BEGIN
 p(y) = y * mp + b_presR
ENDFOR

;=====================================
; Eliminate negative values of RH

FOR s=0,n_elements(rh)-1 DO BEGIN
 IF rh(s) LT 0 THEN rh(s)=0
ENDFOR

;=====================================

b_rhR = rh(0) - mrh * lup
FOR y = ldown, lup-1 DO BEGIN
 relh(y) = y * mrh + b_rhR
ENDFOR

;=====================================
;PASTING ARRAYS

alt=[h,alt]
temp=[t,tair]
pres=[p,pres]
rhum=[relh,rh]


;=======================================
;Fixing dimensions
xx=where(alt lt rfixmax)
d=max(xx)+1

AltR=fltarr(d+1)
TairR=fltarr(d+1)
PresR=fltarr(d+1)
RhR=fltarr(d+1)

FOR i=0,d DO BEGIN
        ;IF (alt(i) LT rfixmax) THEN BEGIN
                AltR(i)=alt(i)

                TairR(i)=temp(i)
                PresR(i)=pres(i)
                RhR(i)=rhum(i)
```

```
        ;ENDIF
    ENDFOR

    END

    ;Program that collocate RaOb data to Radars data to fixed range
    ;Leyda Leon - RUM
    ;Nov/13/2002

    PRO raobcollocate, AltR, TairR, PresR, RhR, range_fixed

    ;RANGE Axis    (114-6084 meters)
    r=200 & range_fixed = IntArr(r) & dr=30 & range_fixed(0)=114
    for j = 1, r-1 do range_fixed(j)=range_fixed(j-1)+dr

    TairR1=TairR

    ;ALIGNING DATA TO FIXED RANGE (114-6054m)

    tmp1=interpol(TairR,AltR,range_fixed)
    tmp2=interpol(PresR,AltR,range_fixed)
    tmp3=interpol(RhR,AltR,range_fixed)

    TairR=tmp1
    PresR=tmp2
    RhR=tmp3

    plot,  Tairr1,  altr  ,linestyle=1,xtitle="Temperature  Raw  RaOb  Data  [C]",
ytitle="Height [m]"
    stop
    oplot,  tairr+1, range_fixed, linestyle=0
    legend, ['Extrapolated','Aligned'], linestyle=[1,0], /top, /left, box=0

    END
```

Program used to retrieve nw,kw2 from Liebe's Model

```
    ; Implimentation of complex Liebe model of the complex refractive index
    ; and dielectric constant of water.
    ; liebe.pro

    ; Leyda Leon - RUM
    ; Nov/13/2002 >>este es para mi data normal

    ; T = temperature [C]
    ; f = frequency [GHz]
    ; fp = pricipal relaxation frequency [GHz]
    ; fs = secondary relaxation frequency [GHz]
    ; e0, e1, e2 = permittivity constants
    ; er = real part of complex permittivity
    ; ei = imaginary part of complex permittivity
    ; nw = complex refractive index of water

    restore, filename="C:\My Documents\LeydaUPRM\Rain\2003\Data2003\raob.dat"    ;para
data normal

    fj=[2.835,94.92]
    Ti=TairR

    nt=n_elements(Ti)
    nf=n_elements(fj)

    nw=ComplexArr(nt,nf)
    Ksqr=fltarr(nt,nf)

    for j=0,nf-1 DO BEGIN  ; FREQUENCY
        for i = 0,nt-1 DO BEGIN       ; TEMPERATURE
```

```
                        f=fj(j)
                        T=Ti(i)

                        theta=300./(T+273.15)
                        e0=77.66 + 103.3*(theta-1.)
                        e1=5.48
                        e2=3.51
                        fs=590. - 1500.*(theta-1.)
                        fp=20.09-142.4*(theta-1.)+294.*(theta-1.)^2.

                        ; temporary variables
                        denom1=1.+(f/fp)^2.
                        denom2=1.+(f/fs)^2.
                        er=(e0-e1)/denom1 + (e1-e2)/denom2 +e2
                        ei=(e0-e1)*(f/fp)/denom1+(e1-e2)*(f/fs)/denom2
                        e=complex(er,-ei)

                        nw(i,j)=sqrt(e)
                        K=(e-1.)/(e+2.)
                        Ksqr(i,j)=abs(K)^2
                ENDFOR
        ENDFOR
        print, 'ya llegue'
        save,                           nw,K,ksqr,                              filename="C:\My
Documents\LeydaUPRM\Rain\2003\Data2003\CRefIndex.dat"       ;para data normal
        stop
END
```

Programs used to align S-band and W-band Radars Data, correct aliasing

```
        ;CORRECT FFT, CORRECT ALIASING, ALIGN DATA, SAVE CORRECT DATA TO WORK WITH
        ;MAR/12/03  using RaOb data
        ;RUM
        ;Leyda Leon

        ;#############################################################################
        RESTORE, FILENAME="F:\LeydaData\W_Band\Wdat\H21Wraw.dat"
        RESTORE, FILENAME="F:\LeydaData\S_Band\Sdat\H21Sraw.dat"
        RESTORE, FILENAME="F:\LeydaData\S_Band\Sdat\H21_fft&V_Sraw.dat"
        RESTORE, FILENAME="F:\LeydaData\S_Band\Sdat\H21S_SNRSraw.dat"
        ;this S-band data doesn't have fft_dataS and v_axisS and SNR_S >> these are
aligned
        ;in other program
        ;#############################################################################
        ;Getting the data as needed

        fft_dataW2=10.^(fft_dataW/10.) ;RAW DATA LINEAL VALUES from [dBm]
        raw_fft=fft_dataW2 ; raw fft data in LINEAL
        linZew=10.^(dBZeW/10.)

        PLOT, v_axisW, fft_dataW2(10,10,*)

        stop

        ;#############################################################################
        ;Correct fft to fit Z values
        correct_fft, timeW, rangesW, fft_dataW2, fw, linZew,v_axisW

        OPLOT, v_axisW, fft_dataW(10,10,*),linestyle=1

        stop

        fft_dataW2=fW ;LINEAL VALUES RANGE CORRECTED

        ;#############################################################################
        ;Correct aliasing
        vami=3
        aliasing,vami,v_axisW, fft_dataW2,timeW,rangesW,una_fft_dataW2,art_doppW
        fft_dataW = una_fft_dataW2 ;LINEAL VALUES ALIAS CORRECTED
```

```
        ;Then una_fft_dataW correspond to the art_doppW axis!!!! REMEMBER!
        ;plot, art_doppW,fft_dataW(10,10,*)


        save, v_axisS, v_axisW, timeW, timeS, rangesW, rangesS , dBZeS, dBZeW, fft_dataW,
fft_dataS,filename="F:\LeydaUPRM\INV_Leyda\Rain\2003\Data2003\Raw_dataCorrected.dat"


        stop

        ;#############################################################################
        ;INTERPOLATION AXES

        ;DOPPLER Axis
        ;Cuando lo hago con art_doppW
        dopp_axis = FltArr(128) & dv=15./128. & dopp_axis(0)=art_doppW(0)
        for j=1,127 do dopp_axis(j)=dopp_axis(j-1)+dV

        ;RANGE Axis    (114-6084 meters)
        r=200 & range_fixed = IntArr(r) & dr=30 & range_fixed(0)=114
        for j = 1, r-1 do range_fixed(j)=range_fixed(j-1)+dr

        ;TIME Axis
        t=355 & dt=10 & time_fixed = LonArr(t) & time_fixed(0)=17
        for j = 1, t-1 do time_fixed(j)=time_fixed(j-1)+dt

        print, "Defined Fixed Arrays"

        ;#############################################################################
        ;FFTBINS Interpolation

        print, "FFT Interpol"
        tmp1 = FltArr(n_elements(timeS),n_elements(rangesS),128)
        tmp2 = FltArr(n_elements(timeW),n_elements(rangesW),128)

        FOR i = 0, n_elements(timeW)-1  do BEGIN
                FOR j = 0, n_elements(rangesW)-1 do BEGIN
                   tmp2(i,j,*)= interpol(fft_dataW(i,j,*), art_doppW, dopp_axis)
                ENDFOR
        ENDFOR
        fft_dataW = tmp2

        FOR i = 0, n_elements(timeS)-1  do BEGIN
                FOR j = 0, n_elements(rangesS)-1 do BEGIN
                   tmp1(i,j,*)= interpol(fft_dataS(i,j,*), v_axisS, dopp_axis)
                ENDFOR
        ENDFOR
        fft_dataS = tmp1

        print, "FFT_DataW & fft_dataS Interpolated"


        ;#############################################################################
        ;TIME INTERPOLATION - this range all times

        print, "Time Interpol... Others"

        ;************************************************** OTHERS
        tmp1 = FltArr(n_elements(time_fixed),n_elements(rangesS))
        tmp2 = FltArr(n_elements(time_fixed),n_elements(rangesW))

        ;REFLECTIVITY
        FOR i = 0, n_elements(rangesS)-1  do BEGIN
           tmp1(*,i)= interpol(dBzeS(*,i), timeS, time_fixed)
        ENDFOR
        dBzeS = tmp1
```

```
FOR i = 0, n_elements(rangesW)-1  do BEGIN
   tmp2(*,i)= interpol(dBzeW(*,i), timeW, time_fixed)
ENDFOR
dBzeW = tmp2

;MEAN VELOCITY
FOR i = 0, n_elements(rangesS)-1  do BEGIN
   tmp1(*,i)= interpol(meanVS(*,i), timeS, time_fixed)
ENDFOR
meanVS = tmp1
FOR i = 0, n_elements(rangesW)-1  do BEGIN
   tmp2(*,i)= interpol(meanVW(*,i), timeW, time_fixed)
ENDFOR
meanVW = tmp2

;SPECTRAL WIDTH
FOR i = 0, n_elements(rangesS)-1  do BEGIN
   tmp1(*,i)= interpol(swS(*,i), timeS, time_fixed)
ENDFOR
swS = tmp1
FOR i = 0, n_elements(rangesW)-1  do BEGIN
   tmp2(*,i)= interpol(swW(*,i), timeW, time_fixed)
ENDFOR
swW = tmp2

;SNRs
FOR i = 0, n_elements(rangesS)-1  do BEGIN
   tmp1(*,i)= interpol(snrS(*,i), timeS, time_fixed)
ENDFOR
snrS = tmp1

FOR i = 0, n_elements(rangesW)-1  do BEGIN
   tmp2(*,i)= interpol(snrW(*,i), timeW, time_fixed)
ENDFOR
snrW = tmp2


;************************************************** SPECTRA
print, "Time Interpol... Spectra"
tmp2 = FltArr(n_elements(time_fixed),n_elements(rangesW),128)

FOR i = 0, n_elements(rangesW)-1  do BEGIN
       FOR j=0, n_elements(dopp_axis)-1 do BEGIN
              tmp2(*,i,j)= interpol(fft_dataW(*,i,j), timeW, time_fixed)
       ENDFOR
ENDFOR
fft_dataW = tmp2

tmp1 = FltArr(n_elements(time_fixed),n_elements(rangesS),128)
FOR i = 0, n_elements(rangesS)-1  do BEGIN
       FOR j=0, n_elements(dopp_axis)-1 do BEGIN
              tmp1(*,i,j)= interpol(fft_dataS(*,i,j), timeS, time_fixed)
       ENDFOR
ENDFOR
fft_dataS = tmp1



;#############################################################################

;RANGE INTERPOLATION - this time all rangesS

;************************************************** OTHERS
print, "Range Interpol... Others"

tmp1 =FLTARR(n_elements(time_fixed), n_elements(range_fixed))
```

```
        tmp2 =FLTARR(n_elements(time_fixed), n_elements(range_fixed))

        ;REFLECTIVITY
        FOR i = 0, n_elements(time_fixed)-1  do BEGIN
           tmp1(i,*)= interpol(dBzeS(i,*), rangesS, range_fixed)
           tmp2(i,*)= interpol(dBzeW(i,*), rangesW, range_fixed)
        ENDFOR
        dBzeS = tmp1
        dBzeW = tmp2

        ;MEAN VELOCITY
        FOR i = 0, n_elements(time_fixed)-1  do BEGIN
           tmp1(i,*)= interpol(meanVS(i,*), rangesS , range_fixed)
           tmp2(i,*)= interpol(meanVW(i,*), rangesW , range_fixed)
        ENDFOR
        meanVS = tmp1
        meanVW = tmp2

        ;SPECTRAL WIDTH
        FOR i = 0, n_elements(time_fixed)-1  do BEGIN
           tmp2(i,*)= interpol(swW(i,*), rangesW, range_fixed)
        ENDFOR
        swW = tmp2

        ;SNRs
        FOR i = 0, n_elements(time_fixed)-1  do BEGIN
           tmp2(i,*)= interpol(snrW(i,*), rangesW, range_fixed)
        ENDFOR
        snrW = tmp2
        FOR i = 0, n_elements(time_fixed)-1  do BEGIN
           tmp1(i,*)= interpol(snrS(i,*), rangesS, range_fixed)
        ENDFOR
        snrS = tmp1


        ;****************************************************** SPECTRA
        print, "Range Interpol... Spectra"

        tmp2 = FltArr(n_elements(time_fixed),n_elements(range_fixed),128)

        FOR i = 0, n_elements(time_fixed)-1  do BEGIN
                FOR j=0, n_elements(dopp_axis)-1 do BEGIN
                        tmp2(i,*,j)= interpol(fft_dataW(i,*,j), rangesW, range_fixed)
                ENDFOR
        ENDFOR
        fft_dataW = tmp2 ;FINAL FFT!!!! [LINEAL VALUES]

        tmp1 = FltArr(n_elements(time_fixed),n_elements(range_fixed),128)
        FOR i = 0, n_elements(time_fixed)-1  do BEGIN
                FOR j=0, n_elements(dopp_axis)-1 do BEGIN
                        tmp1(i,*,j)= interpol(fft_dataS(i,*,j), rangesS, range_fixed)
                ENDFOR
        ENDFOR
        fft_dataS = tmp1

        ;******************************************************

        ;fftx=10.*alog10(fft_dataW/0.001) ;fftx is in [dBm]

        ;plot,v_axisW,fft_dataW2(0,0,*),    xtitle="Doppler    Velocity    Axis    [m/s]",
ytitle="Spectra [dBm]",$
        ;       title="Spectra Vs. Doppler Velocity"
        ;oplot, dopp_axis,fftx(0,0,*), linestyle=2
        ;legend, ['Raw Data','Interpolated'], linestyle=[0,2], /top, /left, box=0


        SAVE    ,  dopp_axis,  range_fixed,  time_fixed,  v_axisW,  fft_dataW,  dBZeW,  meanVW,
```

```
swW, SNRW, $
                      dBzeS,      meanVS,      swS,      SNRS,      v_axisS,      fft_dataS,
FILENAME="F:\LeydaUPRM\INV_Leyda\Rain\2003\Data2003\H21SW_01_ALL.dat"



END
        PRO correct_fft, timeW, rangesW, fft_dataW2, fw, linZew,v_axisW

        ;Spectra Correction
        dVW=0.123459 ;to unscale for velocities
        fW=FltArr(359,160,128)

        factor=FltArr(359,160)
        rw2=(rangesW/1000.)^2.
        cvv=10.^(61.44/10.) ;C=61.44dB radar constant taken from the data file

        ;Looking for the correction factor
        ;Multiplying by the factor
        for t=0,n_elements(timeW)-1 do begin
           for r=0,n_elements(rangesW)-1 do begin
                  factor(t,r)= linZew(t,r) / total(fft_dataW2(t,r,*)*rw2(r)*dVW*cvv)
                  fW(t,r,*)  =    factor(t,r)*fft_dataW2(t,r,*)*rw2(r)*dVW*cvv           ;
[mm^6/m^3 ]
           endfor
        endfor




        print, "fft corrected to Zvalues"

END
        PRO aliasing,vami,v_axisW, fft_dataW2,timeW,rangesW,una_fft_dataW2,art_doppW

        ;Spectra Shifting
        three=min(where(v_axisW gt vami));maximum position where velocities are less than
vami m/s
        span=127-three ;span needed to shift spectra
        d_span=v_axisW(127)-v_axisW(three)
        art_doppW=v_axisW-d_span ;artificial doppler axis

        una_fft_dataW2=FltArr(n_elements(timeW),n_elements(rangesW),128)

        FOR i = 0, n_elements(timeW)-1  do BEGIN
               FOR j = 0, n_elements(rangesW)-1 do BEGIN
                      una_fft_dataW2(i,j,*)=shift(fft_dataW2(i,j,*),span)    ;Shift    the
spectra to unaliase
               end
        end

        print, "Aliasing Corrected"

END
Dual Frequency Method
        ;JAN/2004
        ;Leyda Leon - UPRM
        ;MAIN PROGRAM

        ;Restoring Raw Data Corrected!
        RESTORE,filename="C:\Documents        and        Settings\VANESSA\Desktop\Master's
Research\INV_FINAL\DATA_FINAL\CorrectedData_last.dat"
        ;VARIABLES  AVAILABLE:  lamS,lamW,time_fixed,  range_fixed,  fft_dataW,  fft_dataS,
dBZeW, dBZeS, meanVW, meanVS, swW, swS, factor_ro,$
        ;SNRS, SNRW, ksqr,nw,nt,ng
```

```
        print, 'Defining Arrays'

        Model_RR=FltArr(nt,ng);Rain-Rate Array - using DWR comparison
        Integral_RR=FltArr(nt,ng)  ;Rain-Rate  Array  -  using  Integral  (suitable  for
comparison when using real N(D))
        aveRR_tp=FltArr(nt);time Profile average RainRate using Model of DWR comparison
        VAM_arr=FltArr(nt,ng)
        dBZeSM=FltArr(1,ng) ;dBZeS using Integral of MODEL
        VAM_arr=FltArr(nt,ng)


        print, 'Starting time bins...'

        ;for t=0, 100 do begin ; for all time bins

        ;for t=101, 200 do begin ;

        ;for t=178, 180 do begin ;

        ;for t=201, 354 do begin ;

        ;for t=301,  do begin ;



        ;;for g=0,10 do begin

        ;for g=0,ng-1 do begin ;for all range gates

        ;This  choose  specific  pixels!  Comment  time  varying  for  and  endfor  first  before
using.

        t=166 & g=13
        ;t=156 & g=30 ; low
        ;t=144 & g=16 ;med
        ;t=182 & g=7 ;high

        ;ploting dbz profiles
        !P.MULTI=[0,2,1]
        plot,   dbzes(t,*),   range_fixed/1000.,   xtitle='S-band   Reflectivity   [dB]',
ytitle='Height [m]'
        plot,   dbzew(t,*),   range_fixed/1000.,   xtitle='W-band   Reflectivity   [dB]',
ytitle='Height [m]'

        stop

        ;If there is no data or data is not useful then VAM=!Values.F_NaN and RR=0
        if dbzew(t,g) lt -35.0 then begin

         VAM=0.
         rainrate=0.
         goto, jumpout99

        endif


        ;#############################################################################
        ;Calculates dD/dv from measured data

        Mf=alog((9.25-(dopp_axis*factor_ro(g)))/9.25) ; alog=LN >>9.25 [m/s]
        a=6.8
        b=4.88
        c=Mf
        diam_cm=(-b+sqrt((b^2.)-(4.*a*c)))/(2.*a)  ;Cuadratic  Formula  to  solve  for  the
diameter
        ;^is in[cm]
```

```
        diam=diam_cm*10. ;to change from [cm] to [mm]
        nd=n_elements(diam)

        dv=abs(dopp_axis(1)-dopp_axis(0))
        ddiam=FltArr(n_elements(diam))

        for d=1,nd-1 do begin
            ddiam(d-1)=diam(d)-diam(d-1)
        endfor

        ddiam(nd-1)=ddiam(d-2) ; to be like the last one to have a value
        dDdv_m=ddiam/dv  ;is  the  same  for  W-band  and  S-band  (recall  both  depend  on
dopp_axis)

        ;#############################################################################
        ;Calculates the velocity diameter and so the mie coefficient for the profile's
cell
        vd,  v,  diam,dv,ddiam,g,factor_ro   ;ya tiene el velocity y retorna diam (usa
factor_ro)
        mie_input, g, v, sbs,sbw,ses,sew,diam
        ;#############################################################################

        kw2s=ksqr(g,0) & kw2w=ksqr(g,1)
        DWR_r=dBZeS(t,g)-dbZew(t,g)
        DWR_real=DWR_r

        ;#############################################################################
        ;Calculates DV/DD & DD/DV
        CdDdv,g,diam,factor_ro, dDdv, ddiam, dv  ;(usa factor_ro)
        ;#############################################################################
        ;For all the layers
        factorS=(lamS^4.)/(kw2s*(!pi)^5.) & factorW=(lamW^4.)/(kw2w*(!pi)^5.)
        ;#############################################################################
        ;Calculates DWR_sim1, DWR_sim2
        ;INPUTS: diam, sew, ses,sibw,sibs,dDdv,dv,ddiam,factorS,factorW,g,range_fixed
        ;OUTPUTS: DWR_sim1, DWR_sim2, ratea, ks, kw, Zes, Zew

        DWR, g,ng,nt,t,diam, sew, ses,sbw,sbs,dDdv,dv,ddiam,factorS,factorW,range_fixed,$
               DWR_sim1, DWR_sim2, ratea, ks, kw, Zes1, Zew1,v,cs,cw,mvw,mvs, delta_v

        ;#############################################################################
        ;INPUT: ratea, zew, zes, dwr_sim1, dwr_sim2   OUTPUTS: plots

        ;;plots2, ratea,kw,ks, zew1, zes1, dwr_sim1, dwr_sim2, mvw,mvs,delta_v
        ;;!P.MULTI=[0,1,1] ;para volver las ventanas de plots

        ;stop
        ;#############################################################################
        ;Calculation Rainfall rate for DWR_SIM1 = DWR_REAL
        ;INPUTS: nrr, dwr_real, dwr_sim1, ratea   OUTPUTS: rainrate

        rainfall, dwr_real, dwr_sim2, ratea, rainrate

        ;print, 'Rainrate encontrado = ',rainrate, 'en gate = ',g

        if rainrate eq 0. then begin
        ; print,'hay rr=0 en gate=',g
         VAM=0.
         goto, jumpout99
        endif

        ;#############################################################################
        ;Calculating the Simulated spectra for the 1st cell
        ;INPUTS: rainfall,nr,diam,dd,factor_ro,sibw OUTPUTS: Sw,new_fftW,new_fftS

        sim_spectra, ratea,g,t,rainrate,v, diam, dopp_axis, ddiam, dv, dDdv, $
            sbs, ses, sew, sbw, Sw, k1w, Ss, k1s, fft_dataW, new_fftW, s_fftW,N,$
```

```
            range_fixed,factorS,factorW,fft_dataS,new_fftS,cs,cw,dBZeSM,mvw,mvs,delta_v

        ;#############################################################################
        ;Locates nulls, calculates VAM and shift velocity and data for resulting VAM
        ;INPUTS: g,Sw, v, new_fftW, dopp_axis OUTPUTS: sh_vel, sh_fftW

        null, g, Sw,Ss, v, new_fftW,new_fftS, dopp_axis, sh_vel, sh_fftW, VAM, factor_ro,
diam, dddv_m

        jumpout99:


        ;Calculates rain rate solving integral

        rr, v, rainrate, diam, ddiam, new_RR

        Model_RR(t,g)=rainrate
        Integral_RR(t,g)=new_RR
        VAM_arr(t,g)=VAM

        ;;endfor ;for of varying range-gates

        aveRR_tp(t)=total(model_rr(t,*))/ng ; calculated from model (NOT Integral)

        print, 'Time', t, ' has been completed'


        stop


        IF T EQ 100 THEN BEGIN

        save,  vam_arr,  model_rr,  integral_rr,  averr_tp,  filename="C:\Documents  and
Settings\VANESSA\Desktop\Master's
Research\INV_FINAL\DATA_FINAL\Output\out_data100_last.dat"
        print, 'Data 100 is saved'

        ENDIF

        IF T EQ 200 THEN BEGIN

        save,  vam_arr,  model_rr,  integral_rr,  averr_tp,  filename="C:\Documents  and
Settings\VANESSA\Desktop\Master's
Research\INV_FINAL\DATA_FINAL\Output\out_data200_last_rum.dat"
        print, 'Data 200 is saved'

        ENDIF


        IF T EQ 300 THEN BEGIN

        save,  vam_arr,  model_rr,  integral_rr,  averr_tp,  filename="C:\Documents  and
Settings\VANESSA\Desktop\Master's Research\INV_FINAL\DATA_FINAL\Output\out_data300.dat"
        print, 'Data 300 is saved'

        ENDIF

        IF T EQ 354 THEN BEGIN

        save,  vam_arr,  model_rr,  integral_rr,  averr_tp,  filename="C:\Documents  and
Settings\VANESSA\Desktop\Master's
Research\INV_FINAL\DATA_FINAL\Output\out_data354_last.dat"
        print, 'Data 354 is saved'

        ENDIF

        IF T EQ 180 THEN BEGIN
```

```
        save,  vam_arr,  model_rr,  integral_rr,  averr_tp,  filename="C:\Documents  and
Settings\VANESSA\Desktop\Master's Research\INV_FINAL\DATA_FINAL\Output\out_data_179.dat"
        print, 'Data High is saved'

        ENDIF

        ;endfor ; for of varying time-gates

        print, 'END!!!'


        END
        PRO vd, v, diam,dv,ddiam,g,factor_ro

        nd=250 & diamx=FltArr(nd) & dd=6./nd & diamx(0)=0.1
        for d=1,nd-1 do diamx(d)=diamx(d-1)+dd


        diamx2=diamx/10. ;[cm]
        v=(9.25 - (9.25*exp(-6.8*diamx2^2.-4.88*diamx2)))*factor_ro(g)
        diam=diamx


        ;*************************************************************************
        ;Calculates ddiam
        ddiam = FltArr(n_elements(diam))
        for i=0, n_elements(diam)-1 do ddiam(i)=dd
        ddiam(n_elements(diam)-1)=dd

        ;for i=1, n_elements(diam)-1 do ddiam(i-1)=diam(i)-diam(i-1)
        ;Calculates dv
        dv = FltArr(n_elements(v)) & dv(0)=0
        for i=1, n_elements(v)-1 do dv(i-1)=v(i)-v(i-1)

        dv(n_elements(v)-1)=dv(d-2)
        ;*************************************************************************

        END
        ;PROGRAM TO CALCULATE MIE FORMULATIONS - FIRST LAYER
        ;NOV/13/02
        ;Leyda Leon - RUM
        ;RUN liebe_2003.pro first!!

        ;compile first vd2.pro!!!

        PRO mie_input, g, v, sbs,sbw,ses,sew,diam

        restore,     filename="C:\Documents     and     Settings\VANESSA\Desktop\Master's
Research\INV_FINAL\DATA_FINAL\CRefIndex_2003.dat" ;data normal!!!

        ;************************************
        nwS=nw(g,0) & nwW=nw(g,1)
        kw2s=ksqr(g,0) & kw2w=ksqr(g,1)

        ;************************************
        ;Decidiendo las bandas y sus respectivos valores*************************

        lamS=107.14  & lamW=3.158   ;[mm]
        nd=n_elements(diam)

        ;Definiendo                                                              los
arreglos*****************************************************
        ee=FltArr(nd) & es=FltArr(nd) & ea=FltArr(nd) & eb=FltArr(nd)
        sb=FltArr(nd) & se=FltArr(nd)

        ees=FltArr(nd) & ess=FltArr(nd) & eas=FltArr(nd) & ebs=FltArr(nd)
```

```
        sbs=FltArr(nd) & ses=FltArr(nd)
        eew=FltArr(nd) & esw=FltArr(nd) & eaw=FltArr(nd) & ebw=FltArr(nd)
        sbw=FltArr(nd) & sew=FltArr(nd)

        ;*****************************************************************************
*

        for band=0,1 do begin

        if band eq 0 then m=nwS else m=nwW
        if band eq 0 then lam=lamS else lam=lamW
        if band eq 0 then kw2=kw2s else kw2=kw2w

        nr=float(m) & ni=imaginary(m)
        ;*****************************************************************************
*

        ;V-D relation referenced by Firda (Eqn4) having V we get D:

        xx=!pi*diam/lam & nd=n_elements(diam)

        FOR d=0, nd-1 DO BEGIN ;for all diameters

            x=xx(d) & nmax=round(2.+x+4.*x^(1./3.)) & n=findgen(nmax)+1.
            cn=2.*n+1. & x2=x*x

            an=ComplexArr(nmax)   &      bn=ComplexArr(nmax)   &   A=ComplexArr(nmax)   &
W=ComplexArr(nmax)
            A(0)=1/tan(m*x)

            Wx=complex(cos(x),-sin(x)) & W(0)=complex(sin(x),cos(x))

            FOR i=1, nmax-1 DO BEGIN ;infinite sumatory aproximated to nmax iterations

               ix=i/x & ixm =ix/m & A(i)=(-ixm)+(ixm-A(i-1))^(-1)

               if i eq 1 then W(1)=ix*W(0)-Wx
               if i eq 2 then W(2)=3/x*W(1)-W(0)
               if i ge 3 then W(i)=(((2*i-1)/x)*(W(i-1)))-W(i-2)

               fac1 = A(i)/m + ix & fac2 = A(i)*m + ix
               realWi = float( W(i) ) & realWi1 = float( W(i-1) )

               an(i)=( (fac1*realWi) - (realWi1) )/ ( ( fac1*W(i)) - W(i-1) )
               bn(i)=( (fac2*realWi) - (realWi1) )/ ( ( fac2*W(i)) - W(i-1) )

            ENDFOR

            anp=FLOAT(an) & anpp=IMAGINARY(an) & bnp=FLOAT(bn) & bnpp=IMAGINARY(bn)

            dn=cn*(anp+bnp) & qxx=TOTAL(dn) & qext=2.*qxx/x2
            en=cn*(anp*anp+anpp*anpp+bnp*bnp+bnpp*bnpp)
            qss=TOTAL(en) &  qsca=2.*qss/x2 & qabs=qext-qsca
            fn=cn*(an-bn)   &   gn=(-1.)^n   &   factor=fn*gn   &   qtt=total(factor)   &
qb=abs(qtt)^2./x2

            ee(d)=qext & es(d)=qsca & ea(d)=qabs & eb(d)=qb
            sb(d)=(eb(d)*!pi*diam(d)^2.)/4. & se(d)=(ee(d)*!pi*diam(d)^2.)/4.

        ENDFOR

        if band eq 0 then begin
            ees=ee & ess=es & eas=ea & ebs=eb & sbs=sb & ses=se
        endif

        if band eq 1 then begin
            eew=ee & esw=es & eaw=ea & ebw=eb & sbw=sb & sew=se
```

```
        endif


        ENDFOR

        ;!P.MULTI=[0,1,1] ;para volver las ventanas de plots
        ;window,0
        ;plot, v, sbw, /ylog, xtitle='Velocity [m/s]', ytitle='Backscattering Coefficient
[mm^2]'
        ;oplot, v, sbs, linestyle=1
        ;legend, ['S-band','W-band'], linestyle=[1,0], /top, /left, box=0
        ;window,1
        ;plot, v, sew, /ylog, xtitle='Velocity [m/s]', ytitle='Extinction Coefficient
[mm^2]'
        ;oplot, v, ses, linestyle=2



        END
        ;Program that calculates the DWR_sim1 and DWR_sim2
        ;Leyda Leon
        ;12/Mar/2003 - RUM


        pro                   DWR,                   g,ng,nt,t,diam,                    sew,
ses,sbw,sbs,dDdv,dv,ddiam,factorS,factorW,range_fixed,$
               DWR_sim1, DWR_sim2, ratea, ks, kw, Zes1, Zew1,v,cs,cw,mvw,mvs, delta_v

        ;*****************************************************************
        ; Declaring Arrays

        nd=n_elements(diam) ;xxs=xxw rs=rw they have the same number of elements
        RateA=findgen(1000)*0.1+0.1 ; Rain-Rates from 0.1 to 100 mm/hr
        nr=n_elements(RateA)

        N=FltArr(nd) & Z1s=FltArr(nd) & Z1w=FltArr(nd) & k1s=FltArr(nr)
        k1w=FltArr(nd) & Sw=FltArr(nd) & Ss=FltArr(nd)

        mvw=FltArr(nr) & mvs=FltArr(nr)
        i1w=FltArr(nd) & i2w=FltArr(nd)
        i1s=FltArr(nd) & i2s=FltArr(nd)

        delta_v=FltArr(nr)

        Zes=FltArr(nr) & Zew=FltArr(nr) & ds=FltArr(nr) & dw=FltArr(nr)
        Ks=FltArr(nr) & Kw=FltArr(nr)

        DWR_sim1=FltArr(nr) & DWR_sim2=FltArr(nr)


        FOR r=0L, nr-1L DO BEGIN ;For all rain-rates

            FOR d=0, nd-1 DO BEGIN ;For all diameters

               N(d)=8e3*exp(-4.1*(RateA(r)^(-0.21))*diam(d))  ;function of the diameter...
diam is in[mm]

               ;ATENUATIONS

               k1s(d) = N(d)*ses(d)*ddiam(d) & k1w(d) = N(d)*sew(d)*ddiam(d)

               ;SPECTRA :solving the inside elements of the integral (*dv(i))
               Ss(d) = N(d)*sbs(d)*dDdv(d)*dv(d)/1000.
               Sw(d) = N(d)*sbw(d)*dDdv(d)*dv(d)/1000.

            ;MEAN VELOCITY
            ;W-band mean velocity
```

```
            i1w(d)=N(d)*sbw(d)*v(d)*ddiam(d)
            i2w(d)=N(d)*sbw(d)*ddiam(d)

            ;S-band mean velocity
            i1s(d)=N(d)*sbs(d)*v(d)*ddiam(d)
            i2s(d)=N(d)*sbs(d)*ddiam(d)


            ENDFOR

            ;Mean Velocity
            mvw(r)=total(i1w)/total(i2w)
            mvs(r)=total(i1s)/total(i2s)
            delta_v(r)=mvs(r)-mvw(r)

            ;not in  dB >> mm^6 m^-3
            Zes(r)=factorS*TOTAL(Ss) ;Solving integral
            Zew(r)=factorW*TOTAL(Sw)

            ;if ratea(r) gt  5 then stop

            ;DWR without eliminating atenuation
            DWR_sim1(r) = 10.*alog10(Zes(r) / Zew(r))  ;1st divide them and the change to
dB

            ;k is the attenuation at that cell 30=drange 2 because is two way
            Ks(r) = 2. * 4.34 * TOTAL(k1s) * 1e-6 * 30.*(g+1)    ; [dB] with sigma in mm^2
            Kw(r) = 2. * 4.34 * TOTAL(k1w) * 1e-6 * 30.*(g+1) ; the 1e-6 is the factor
used because D[mm]

            ;c1 is the attenuation between the radar and the first cell
            ds(r) = 10.*alog10(Zes(r)) - Ks(r)  ;Both in dB
            dw(r) = 10.*alog10(Zew(r)) - Kw(r)


            ;DWR with x meters of atenuation
            DWR_sim2(r) = ds(r) - dw(r)

            ;DWR_sim1 = without removing attenuation
            ;DWR_sim2 = removing attenuation

        ENDFOR

        ZeS1=ds ;is in [dB] and atmospheric attenuation removed
        ZeW1=dw

        END
        ;REFLECTIVITIES AND DWRs PLOTS VS RAIN RATE FOR THE 1ST CELL!!!
        ;INPUT: ratea, zew, zes, dwr_sim1, dwr_sim2   OUTPUTS: plots
        ;Leyda Leon - RUM
        ;Mar/12/2003


        PRO plots2, ratea, kw, ks, zew1, zes1, dwr_sim1, dwr_sim2, mvw,mvs,delta_v

        window, xsize=1000, ysize=700

        !P.MULTI=[0,2,2]
        plot, ratea, kw, /xlog, /ylog, xtitle="Rain-Rate [mm/hr]", ytitle="Ättenuation
[dB/m]", yrange=[1e-5,1e2]
        oplot, ratea, ks, linestyle=1
        legend, ['W-band','S-band'], linestyle=[0,1], /top, /left, box=0

        plot, ratea, dwr_sim2, /xlog, xtitle="Rain-Rate [mm/hr]", ytitle="DWR [dB]";,
xrange=[0.1,10]
        oplot, ratea, dwr_sim1, linestyle=1
        legend, ['Removing Attenuation','No Attenuation Removed'], linestyle=[0,1], /top,
```

```
/left, box=0

       plot,    ratea,    ZeS1,    linestyle=1,    /xlog,    xtitle="Rain-Rate    [mm/hr]",
ytitle="Reflectivity [dB]";, xrange=[0.1,10]
       oplot, ratea, ZeW1, linestyle =0
       legend, ['S-band','W-band'], linestyle=[1,0], /top, /left, box=0

       plot,  ratea,  mvs,  linestyle=1,  /xlog,  xtitle="Rain-Rate  [mm/hr]",  ytitle="Mean
Velocity [m/s]"
       oplot, ratea, mvw, linestyle =0
       legend, ['S-band','W-band'], linestyle=[1,0], /top, /left, box=0

       window,2,xsize=1000, ysize=700
       !P.MULTI=[0,2,2]

       plot,  ratea,  delta_v,  /xlog,  xtitle="Rain-Rate  [mm/hr]",  ytitle="Differencial
Velocity [m/s]"

       ;window,2
       ;plot,   dwr_sim2,   zes1,   psym=2,   ytitle="Modeled   DWR   [dB]",   xtitle="S-band
Reflectivity [dB]"
       ;window,3
       ;plot,   dwr_sim2,   zew1,   psym=2,   ytitle="Modeled   DWR   [dB]",   xtitle="W-band
Reflectivity [dB]"

       END
       ;Calculation Rainfall rate for DWR_SIM1 = DWR_REAL
       ;INPUTS: nrr, dwr_real, dwr_sim1, ratea   OUTPUTS: rainfall
       ;Leyda Leon - RUM
       ;Oct/25/2002

       PRO rainfall, dwr_real, dwr_sim2, ratea, rainrate

       nr=n_elements(ratea)

       FOR r=1L, nr-1L DO BEGIN ;For all rain-rates
              IF DWR_sim2(r) gt DWR_real THEN BEGIN

                x=dwr_real
                x1=dwr_sim2(r)
                x2=dwr_sim2(r-1)
                y1=ratea(r)
                y2=Ratea(r-1)

                rainrate=((y2-y1)/(x2-x1)*(x-x2))+y2
                goto, jumpout1
              ENDIF
              rainrate=0 ;if there is no comparison then rainrate=0
       ENDFOR

       jumpout1: ;Get out of the FOR and does not continue calculating DWRs!!!


       END
       ;Program to verify nulls...
       ;Oct/15/2002
       ;Leyda Leon - RUM

       ;START.....rutine  to  calculate  the  first  minimum  after  the  first  maximun  of
new_fftW
       PRO  null,  g,  Sw,Ss,  v,  new_fftW,new_fftS,  dopp_axis,  sh_vel,  sh_fftW,  VAM,
factor_ro, diam, dddv_m

       ;Evaluates the rgate cell
       temp1=Sw &  temp2=new_fftW

       ;Defining Arrays
```

```
        n_sw=n_elements(temp1)  & n_fft=n_elements(temp2)

        max1=max(temp1) & map1x=where(temp1 eq max1)+1 ;Simulated spectra maximum and its
position
        map1=map1x(0)
        max2=max(temp2) & map2x=where(temp2 eq max2)+1 ;Measured spectra maximum and its
position
        map2=map2x(0)

        ;Locates the Simulated Spectra first minimum
        i=map1

        while (i le n_sw-1) do begin
            ;print, 'entre aqui'
            if temp1(i) gt temp1(i-1) then begin
               mip_sim=i-1  &    goto, jumpout3
            endif
            i=i+1
        endwhile
        jumpout3:

        ;Locates the Measured Spectra first minimum
        i=map2
        while (i le n_fft-1) do begin
            if temp2(i) gt temp2(i-1) then begin
               mip_mea=i-1 &  goto, jumpout4
            endif
            i=i+1
            if i eq n_fft-1 then begin
               VAM=0.
               goto, jumpout5
            endif
        endwhile
        jumpout4:

        ;Calculates the VAM
        VAM = v(mip_mea) - v(mip_sim)

        ;Print, 'Vam= ',VAM

        jumpout5:

        ;Changes from dopp_axis to vel_axis
        vel_axis=dopp_axis

        ;Shift velocity axis by VAM lag
        sh_vel=FltArr(n_elements(vel_axis))
        for i=0, n_elements(sh_vel)-1 do sh_vel(i)= vel_axis(i) - VAM ;remove VAM from
vel_axis

        ;Shift Spectra by VAM lag with new velocity axis
        sh_fftW=new_fftW ;but corresponding to sh_vel

        last_vel_axis=sh_vel
        ;*****************************************************************************
*******
        ;print,'VAM=', vam
        ;Plots to see shifted and not shifted measured spectra

        ;window,2
        plot, sh_vel, sh_fftW, xtitle='Shifted Velocity Axis [m/s]', ytitle='Spectras
[mm2m-3/m*s-1]'
        oplot, vel_axis, new_fftW, linestyle=1
        legend, ['Shifted Spectra','Old Spectra'], linestyle=[0,1], /top, /right, box=0
        ;stop
        END
```